Molecular Microbiology (2011) 81(2), 415–433 ■
doi:10.1111/j.1365-2958.2011.07701.x
First published online 31 May 2011

Aberrant protein *N*-glycosylation impacts upon infection-related growth transitions of the haploid plant-pathogenic fungus *Mycosphaerella graminicola*

Juliet Motteram,[1] Alison Lovegrove,[3] Elizabeth Pirie,[1] Justin Marsh[3], Jean Devonshire,[1,2] Allison van de Meene,[1,2] Kim Hammond-Kosack[1] and Jason J. Rudd[1]*

[1]*Department of Plant Pathology and Microbiology,* [2]*Rothamsted Centre for Bioimaging,* [3]*Department of Plant Science, Rothamsted Research, Harpenden, Herts AL5 2JQ, UK.*

Summary

The ascomycete fungus *Mycosphaerella graminicola* is the causal agent of Septoria Tritici Blotch disease of wheat and can grow as yeast-like cells or as hyphae depending on environmental conditions. Hyphal growth is however essential for successful leaf infection. A T-DNA mutagenesis screen performed on haploid spores identified a mutant, which can undergo yeast-like growth but cannot switch to hyphal growth. For this reason the mutant was non-pathogenic towards wheat leaves. The gene affected, *MgAlg2*, encoded a homologue of *Saccharomyces cerevisiae* ScAlg2, an alpha-1,2-mannosyltransferase, which functions in the early stages of asparagine-linked protein (*N*-) glycosylation. Targeted gene deletion and complementation experiments confirmed that loss of *MgAlg2* function prevented the developmental growth switch. *MgAlg2* was able to functionally complement the *S. cerevisiae* ScAlg2-1 temperature sensitive growth phenotype. Spores of ΔMgAlg2 mutants were hypersensitive to the cell wall disrupting agent Calcofluor white and produced abnormally hypo-*N*-glycosylated proteins. Gene expression, proteome and glycoproteome analysis revealed that ΔMgAlg2 mutant spores show responses typically associated with the accumulation of mis-folded proteins. The data presented highlight key roles for protein *N*-glycosylation in regulating the switch to hyphal growth, possibly as a consequence of maintaining correct folding and localization of key proteins involved in this process.

Accepted 4 May, 2011. *For correspondence. E-mail jason.rudd@bbsrc.ac.uk; Tel. (+44) 582 763133 ext 2187; Fax (+44) 582 760981.

Introduction

Pathogenic fungi undergo various developmental changes in order to infect their hosts. A particular group is referred to as dimorphic, which describes an ability to switch between a yeast-like budding growth state and a filamentous, hyphal growth state. Transitions between the two often occur in response to changing environmental stimuli, including temperature and nutritional status. With respect to fungal pathogens of animals in particular, the triggers that signal these growth state transitions have been well studied, as have the signalling pathways that underpin these developmental changes (Lengeler *et al.*, 2000; Borges-Walmsley *et al.*, 2002; Woods, 2002; Nemecek *et al.*, 2006; Whiteway and Bachewich, 2007). For many well-studied dimorphic fungal pathogens of animals the pathogenic (or infectious) state is often the yeast-like form, which may aid the propagation and spread of the organism throughout the vascular system of the host (Rappleye and Goldman, 2006; Klein and Tebbets, 2007).

Dimorphic fungal pathogens are also responsible for some important diseases of cereal crop plants (Nadal *et al.*, 2008). Arguably, the best studied fungal pathogen of this type is the basidiomycete *Ustilago maydis*, the causal agent of corn smut disease. *U. maydis* is non-pathogenic towards its host in the yeast-like growth phase, but becomes pathogenic following the transition to hyphal growth after the fusion of two haploid sporidia which generate the dikaryotic infection hyphae. The complex molecular interplay, which underpins this morphological transition, has been the subject of intensive research (Ruizherrera *et al.*, 1995; Sanchez-Martinez and Perez-Martin, 2001; Kamper *et al.*, 2006; Klosterman *et al.*, 2007; Nadal *et al.*, 2008). Less well studied are the dimorphic ascomycete cereal-infecting fungi, which include *Mycosphaerella graminicola* (anamorph *Septoria tritici*), the causal agent of Septoria Tritici Blotch (STB) disease of wheat. *M. graminicola* can infect wheat leaves in its haploid form through the spread of asexual spores.

These spores are frequently multicellular, often composed of one to four cells. A prerequisite for infection however is the ability of these yeast-like spores to form hyphae on the leaf surface. This occurs rapidly upon contact with wheat leaves (Mehrabi *et al*., 2006) and represents an essential transition, as *M. graminicola* penetrates leaves almost exclusively via hyphal growth through stomatal apertures (Kema *et al*., 1996). The fungal hyphae then continue to grow intercellularly within the leaf in an asymptomatic manner for up to ~ 9 days. Thereafter disease symptoms appear in the form of necrotic leaf lesions, which appear to result from the activation of a host programmed cell death (PCD) response (Keon *et al*., 2007; Rudd *et al*., 2008). The fungus then appears to respond to the increased availability of nutrients released from dying plant cells with the development of asexual sporulation structures (pycnidia) and the synthesis of more asexual spores. These spore (or conidia) masses emerge from stomata and are subsequently propagated by rain splash throughout the wheat canopy. But they must then go through the same developmental processes on un-infected leaf tissues, again requiring the transition into hyphae on the leaf surface. Although it may be argued that most, if not all, plant pathogenic fungi require this initial step, *M. graminicola* is somewhat unusual as these morphological growth transitions are influenced by environmental changes, and can be easily mimicked *in vitro*. For example, *M. graminicola* spores will preferentially replicate by yeast-like conidial budding on rich nutrient media and/or at 15°C. In contrast *M. graminicola* spores will differentiate into filamentous hyphae in poor nutrient conditions (which may mimic the leaf surface) and at higher temperatures (~ 25°C). Therefore, this fungus can display both environmental and temperature-sensitive morphological growth changes characteristic of dimorphic fungi. However, for *M. graminicola*, it is the filamentous growth state that is actively pathogenic towards the plant enabling stomatal penetration and intercellular leaf colonization.

To date only one gene has been implicated in regulating the transition from yeast-like to hyphal growth of *M. graminicola*, the *MgHog1* mitogen-activated protein kinase. Mutant strains disrupted at *MgHog1* were able to proliferate by yeast-like budding but were unable to differentiate hyphae under favourable conditions, including the wheat leaf surface. For this reason these MgHog1 mutant strains were non-pathogenic despite being viable in the yeast-like form (Mehrabi *et al*., 2006). Thus the importance of the yeast to hyphal transition for *M. graminicola* pathology highlights a potential disease control intervention point for STB disease, and the mechanisms underpinning this process merit further study.

Many eukaryotic proteins associated with the cell wall, or secreted from cells, are frequently glycosylated either on asparagine (*N*-linked glycosylation) or on serine/threonine (*O*-linked glycosylation). These modifications support essential functions, which include ensuring correct protein folding and localization. Fungi and animals possess an *O*-linked protein glycosylation pathway not found in plants which involves the direct addition of mannose to proteins in a process known as *O*-mannosylation (Strahl-Bolsinger *et al*., 1999; Lommel and Strahl, 2009). In contrast, the early 'core' pathway of protein *N*-glycosylation is considered to be largely conserved across all studied eukaryotes, but has been most extensively studied in the diploid yeast *Saccharomyces cerevisiae* (Burda and Aebi, 1999; Lehle *et al*., 2006). *N*-linked glycosylation begins with a series of sequential reactions, which occur initially on the cytosolic face, and then within the lumen, of the endoplasmic reticulum (ER). These steps involve the activity of various (ER) membrane-associated proteins leading to the construction of a dolichol-pyrophosphate (Dol-PP) linked 14-sugar 'core' glycan structure Dol-PP-(*N*-acetylglucosamine)$_2$Mannose$_9$Glucose$_3$. This is transferred by an oligosaccharide transferase complex to asparagine side-chains present in an Asn-x-Ser/Thr sequon motif of the target proteins, and is further modified in both the ER and the Golgi apparatus (Helenius and Aebi, 2001). The assembly of this core structure in *S. cerevisiae* involves the sequential function of the *Alg* (*asparagine-linked glycosylation*) genes (Huffaker and Robbins, 1982; 1983). These encode a variety of enzymatic functions including many glycosyltransferases which have been shown, or predicted to be embedded in, or attached to, the ER membrane (Burda and Aebi, 1999; Lehle *et al*., 2006). In *S. cerevisiae* complete loss of function of many *Alg* genes is lethal; therefore many studies aimed at defining the core pathway of *N*-glycosylation have used temperature sensitive alleles of *Alg* genes (Huffaker and Robbins, 1982; 1983; Reiss *et al*., 1996; Kampf *et al*., 2009). The importance of correct protein *N*-glycosylation in eukaryotes is particularly emphasized by the range of congenital diseases of humans, which have been shown to result from defects in the synthesis of the core glycan structure (Freeze and Aebi, 2005; Lehle *et al*., 2006; Jaeken and Matthijs, 2007). This important system of post-translational modification hence impacts upon many aspects of cellular function ranging from correct protein secretion to regulation of the cell cycle (Kukuruzinska and Lennon, 1994; Lennon *et al*., 1997; Helenius and Aebi, 2001). Despite this, to date comparably little research has been performed on the protein *N*-glycosylation pathway in filamentous fungi, which has been predicted to have features in common with, as well as differences, to humans and budding yeasts (Deshpande *et al*., 2008).

The present study was initiated following the identification of a non-pathogenic haploid strain of *M. graminicola*, which was recovered from a T-DNA mutagenesis forwards genetic screen. The T-DNA insertion was mapped to a

putative sequence homologue of the *S. cerevisiae Alg2* mannosyltransferase, which catalyses the conversion of Dol-PP-$(GlcNAc)_2Mann_1$ through to Dol-PP-$(GlcNAc)_2Mann_3$ in the early stages of assembly of the core glycan structure (Jackson *et al*., 1993). The *M. graminciola* Alg2 mutant (ΔMgAlg2) was unable to infect susceptible wheat leaves due to an inability to switch from yeast-like budding to filamentous growth. The data presented here highlight the critical importance of protein *N*-glycosylation for infectious hyphal growth of *M. graminicola*, but also demonstrate that yeast-like growth can occur despite major perturbations to this process.

Results

Identification of a non-pathogenic mutant of M. graminicola *unable to switch from budding yeast-like growth to infectious hyphal growth*

A non-pathogenic T-DNA insertion mutant, referred to as 5-29H, was identified via an attached wheat leaf bioassay (Keon *et al*., 2007) during an initial screen of 615 transformed strains. At 21 days following inoculation, the wild-type strain induced localized leaf cell death, resulting in the formation of necrotic areas bearing asexual sporulation structures (pycnidia – Fig. 1A). In contrast,

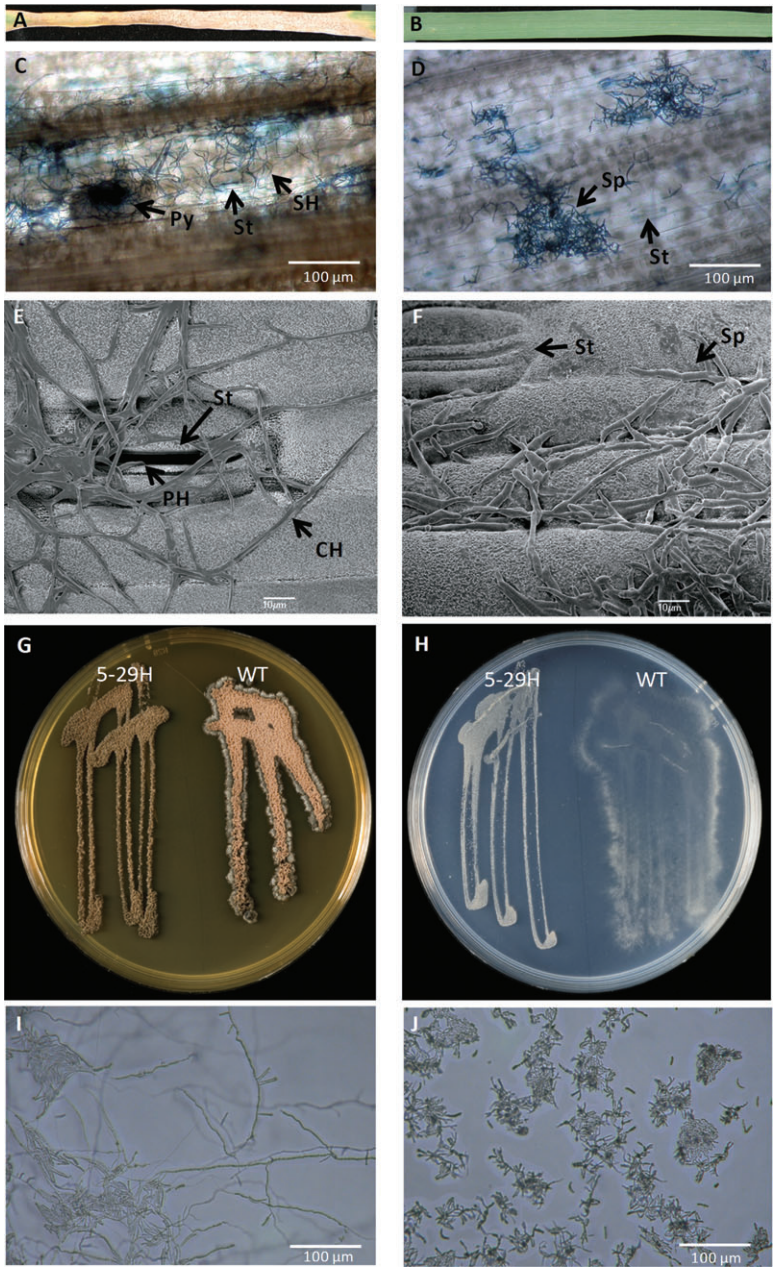

Fig. 1. Identification of a non-pathogenic *M. graminicola* mutant 5-29H unable to switch from budding yeast-like growth to infectious hyphal growth.
A. Wheat leaf 21 days after inoculation with the wild-type fungus. The leaf appears fully necrotic and harbours fungal asexual sporulation (pycnidia) structures.
B. Wheat leaf 21 days after inoculation with the T-DNA insertion mutant 5-29H.
C. Trypan blue stained wild-type fungus 21 days after leaf inoculation. The abbreviation Py highlights the presence of a pycnidium; St highlights a stomatal aperture; SH indicates surface hyphae.
D. Trypan blue stained fungal mutant 5-29H, 21 days after leaf surface inoculation; abbreviation St highlights a stomatal aperture; Sp indicates un-germinated spores.
E. Scanning electron micrograph (SEM) of the wild-type fungus four days after leaf surface inoculation. Abbreviation CH indicates collapsed hypha; PH indicates leaf penetrating hypha.
F. SEM of the 5-29H mutant fungus four days after leaf surface inoculation. Indicated abbreviations as in (D).
G. Macroscopic growth of wild-type and 5-29H mutants on YEPD plate 10 days after inoculation.
H. Macroscopic growth of wild-type and 5-29H mutants on tap water agar (TWA) plates after 10 days.
I. Hyphal growth of the wild-type strain on TWA visualized by light microscopy.
J. The failure of the 5-29H mutant to produce filamentous hyphae on TWA again visualized by light microscopy.

Fig. 2. The 5-29H mutant has a T-DNA insertion within a predicted *Alg2*-like mannosyltransferase gene which functionally complements the yeast (*Saccharomyces cerevisiae*) Alg2-1 temperature sensitive growth phenotype.
A. Diagram illustrating the roles of the *S. cereviseae* Alg proteins in the early endoplasmic reticulum (ER)-associated stages of protein *N*-glycosylation, leading to attachment of the core glycan structure, Dol-PP-(N-acetylglucosamine)$_2$Mannose$_9$Glucose$_3$. The reaction(s) performed by Alg2 are indicated in large bold font.
B. Amino acid alignment of MgAlg2 with ScAlg from *Saccharomyces cerevisiae*. Lines indicate the presence of the conserved predicted glycosyltransferase domain. The position of a conserved Lysine residue at position 230 which is critical for the function of ScAlg2 is highlighted by an asterisk (*). The position of the T-DNA left border insertion is indicated by the arrow.
C. PCR on genomic DNA suggested that T-DNA integration may have triggered a re-arrangement or deletion event at the *MgAlg2* locus. Upper panel indicates the position of PCR primers (P1 and P2) relative to the T-DNA insertion. Lower panel shows the result of PCR on genomic DNA from wild-type and 5-29H mutant fungus. *MgSOD1* (superoxide dismutase 1) primers were used as a control for the quality of the genomic DNA.
D. TMHMM prediction of transmembrane (TM) helices in the MgAlg2 and ScAlg2 proteins.
E. Yeast functional complementation assay. Both the full-length and a truncated version of MgAlg2, omitting the coding sequence for the c-terminal predicted TM domain, were able to restore growth of the temperature sensitive ScAlg2-1 strain at 34°C.

leaves inoculated with mutant 5-29H showed no disease symptoms whatsoever at this time point (Fig. 1B) or at any point thereafter (monitored for over 40 days post inoculation).

Trypan blue staining of inoculated leaves was performed to determine whether the 5-29H pathogenicity defect occurred pre- or post-stomatal penetration. In contrast to the extensive hyphal growth seen on the surfaces and throughout leaves infected by the wild-type strain (Fig. 1C), no extended hyphal filaments were produced by 5-29H on the leaf surface (Fig. 1D). Scanning electron microscopy performed 4 days after leaf surface inoculation emphasized a dramatic difference in the development of the wild-type and 5-29H mutant strains. In contrast to the wild-type strain, which had numerous (often collapsed) surface hyphae frequently penetrating stomata (Fig. 1E), the 5-29H mutant remained in the form of un-germinated spores (Fig. 1F). No extended hyphal filaments were observed whatsoever for this mutant. These data suggested that 5-29H was defective in the pre-penetrative growth phase of colonization of wheat leaves, due to an inability to differentiate hyphae required to penetrate stomata on the leaf surface.

We tested whether the failure of hyphal growth by mutant 5-29H was strictly associated with growth on the leaf surface or whether this was a more general developmental defect, which might also be detected *in vitro*. The 5-29H mutant was inoculated alongside the wild-type strain on both rich nutrient agar [yeast extract peptone dextrose (YEPD); Fig. 1G] and on tap water agar (TWA), the latter of which stimulates significant hyphal growth by the wild-type strain (Fig. 1H). While both strains grew at similar rates during budding yeast-like growth on rich medium, the 5-29H mutant was unable to generate hyphal filaments on TWA (Fig. 1I and 1J). These data suggest that the 5-29H mutant is unable to cause disease on wheat leaves due to a developmental defect in the ability of spores to form hyphae required for leaf penetration.

The 5-29H mutant possesses a T-DNA insertion in a gene encoding a homologue of the Saccharomyces cerevisiae *alpha mannosyltransferase gene,* ScAlg2

We performed thermal asymmetric interlaced PCR (TAIL-PCR) on genomic DNA isolated from the 5-29H mutant strain in order to identify the region harbouring the T-DNA insertion. Three sequences retrieved from independent PCR products harbouring Left Border T-DNA were used in a Blastn search against the sequenced *M. graminicola* genome (http://genome.jgi-psf.org/Mycgr3/Mycgr3.home.html). All sequences returned the same hit (at e-0) on chromosome 9 of the genome with a gene model Id; estExt_Genewise1Plus.C_chr_90094. This predicted gene of 1515 base pairs (bp) containing an open reading frame (ORF) of 1437 bp encoded a protein of 479 amino acids. The left border T-DNA insertion occurred at nucleotide position 1334 bp of the predicted ORF. Blastp analysis against the NCBI non-redundant protein database (http://www.ncbi.nlm.nih.gov/blast/Blast.cgi) with the encoded protein identified homologues annotated as belonging to the yeast (*Saccharomyces cerevisiae*) Alg2 class of Group 1 glycosyltransferases. Blastp analysis against the *S. cerevisiae* genome database (http://www.yeastgenome.org/) returned the protein ScAlg2 with most similarity (1.1e-83). The *M. graminicola* genome browser annotation also suggested that this ORF may encode a Group 1 glycosyltransferase belonging to the yeast Alg2 class, potentially involved in the assembly of the Dol-PP-(GlcNAc)$_2$Mann$_9$Gluc$_3$ core structure for eukaryotic protein *N*-glycosylation (Fig. 2A). We refer to this gene hereafter as *MgAlg2*.

Alignment of MgAlg2 with ScAlg2 highlighted the presence of a conserved glucosyltransferase domain possessing a conserved Lysine (K) in an equivalent position to K230 of ScAlg2 (indicated by an asterisk* in Fig. 2B), which is essential for protein function (Kampf *et al.*, 2009). The left border T-DNA insertion in the original 5-29H mutant was determined to have occurred within the coding region for amino acids 445–446, a position 30 residues from the

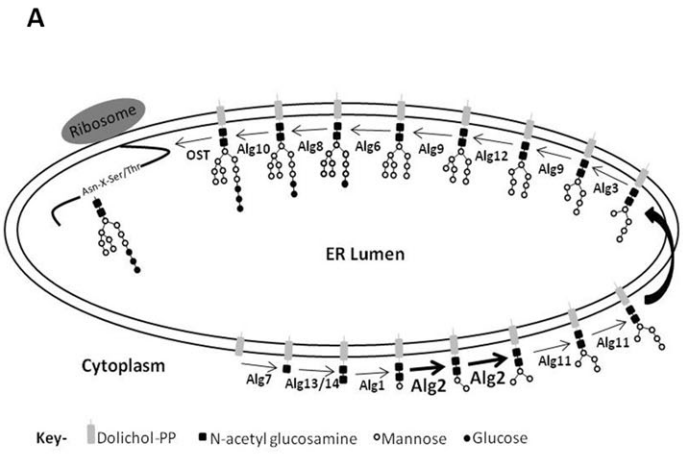
A
Ribosome
OST
Asn-X-Ser/Thr
Alg10
Alg8
Alg6
Alg9
Alg12
Alg9
Alg3
ER Lumen
Cytoplasm
Alg7
Alg13/14
Alg1
Alg2
Alg2
Alg11
Alg11
Key-
Dolichol-PP
N-acetyl glucosamine
Mannose
Glucose

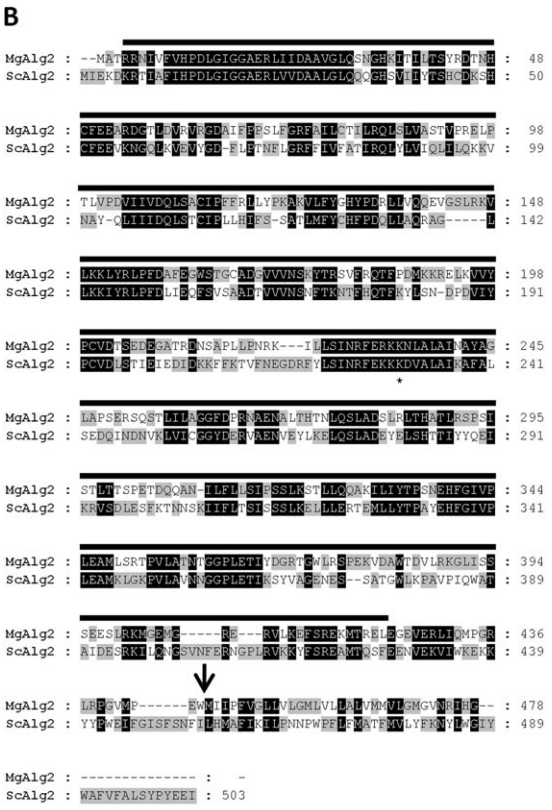
B
MgAlg2 : --MATRRNIVFVHPDLGIGGAERLIIDAAVGLQSNGHKITIITSYRDTNH : 48
ScAlg2 : MIEKDLKRTIAFIHPDLGIGGAERLVVDAALGLQQQGHSVHIYTSHCDKSH : 50
MgAlg2 : CFEEARDGTLDVRVRGDAIFPSLFGRFAILCTILRQLSLVASTVPRELP : 98
ScAlg2 : CFEEVKNGQLKVWVYGL-ELPTNELGRFFIVFATIRQLYLVIQLLQKKV : 99
MgAlg2 : TLVPDVIIVDQLSACIEFFRLLYPKAKVLFYGHYPERLIVQQEVGSLRKV : 148
ScAlg2 : NAY-QLIIIDQLSTCIELLHIFS-SATLMFYGHFPDQLLAQRAG-----L : 142
MgAlg2 : LKKLYRLPFDAFEEWSTGCADGVVVNSKYTRSVGRQTFPDMKKRELKVVY : 198
ScAlg2 : LKKIYRLPFDLIEQFSVSAALTVVVNSNFTKNTFHQTFKYLSN-DPDVIY : 191
MgAlg2 : PCVDTSEDEGATRENSAPLLPNRK---ILLSINRFERKKNLALAIKAYAG : 245
ScAlg2 : PCVDLSTIEIEDIKKFFKTVENEGDRFYLSINRFEKKKDVALAIKAFAL : 241
MgAlg2 : LAPSERSQSTLILAGGFDERNAENALTHTNLQSLAESLRLTHATLRSFSI : 295
ScAlg2 : SEDQINDNVKLVICGGYDERVAENVEYLKELQSLAEGYELSHTTIYYQEI : 291
MgAlg2 : STLTTSPETDQQAN-ILFLLSIESSLKSTLLQQAKILIYTESNSHFGIVP : 344
ScAlg2 : KPVSDLESFKTNNSKIIFLTSISSLKELLLERTEMLLYTPAYSHFGIVP : 341
MgAlg2 : LEAMLSRTPVLATNTGGPLETIYDGRTGWLRSPEKVDAWTDVLRKGLISS : 394
ScAlg2 : LEAMKLGKPVLAVNNGGPLETIKSYVAGENESS--SATGWLKPAVPIQWAT : 389
MgAlg2 : SEESLRKMGEMG-----RE---RVLKEFSREKMTRELESEVERLIQMPGR : 436
ScAlg2 : AIDESRKILQNGSVNFERNGPLRVKKYFSREAMTQSFENVEKVIWKEKK : 439
MgAlg2 : LPEGVMP------EWMTIPEVSLIVLGMLVLLALVMMVLSMGVNRHHG-- : 478
ScAlg2 : YYEWEIFGISFSNFILHMAFIKILPNNPWPELPSMATFMVLYFKNYLMGIY : 489
MgAlg2 : ---------- : -
ScAlg2 : WAFVFALSYPYEEI : 503

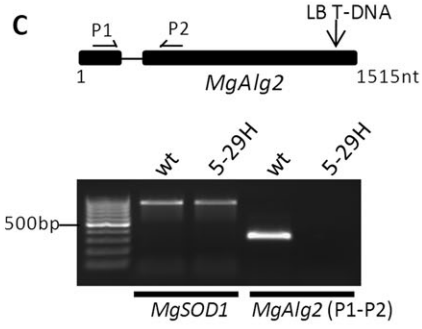
C
P1
P2
LB T-DNA
1
MgAlg2
1515nt
wt
5-29H
wt
5-29H
500bp
MgSOD1
MgAlg2 (P1-P2)

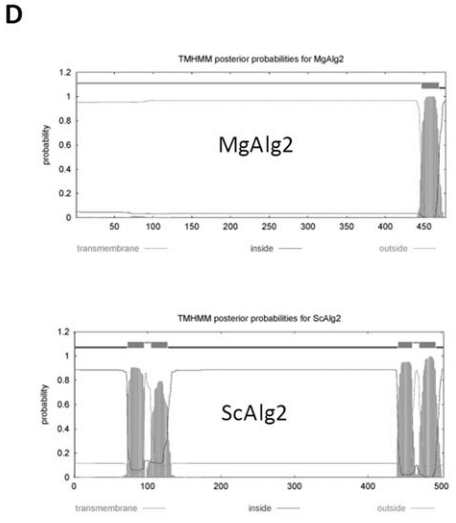
D
TMHMM posterior probabilities for MgAlg2
MgAlg2
probability
transmembrane
inside
outside
TMHMM posterior probabilities for ScAlg2
ScAlg2
probability
transmembrane
inside
outside

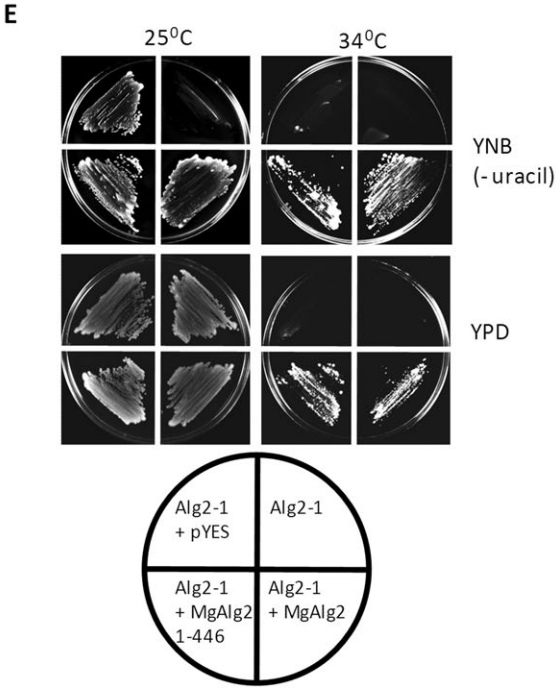
E
25⁰C
34⁰C
YNB
(-uracil)
YPD
Alg2-1
+ pYES
Alg2-1
Alg2-1
+ MgAlg2
1-446
Alg2-1
+ MgAlg2

C-terminus of the protein (indicated by an arrow in Fig. 2A). However, PCR on genomic DNA directed towards the 5′ end of the *MgAlg2* gene (between nucleotides 78–323) failed to amplify a product from the 5-29H mutant (Fig. 2C) suggesting that a deletion or re-arrangement event may have occurred at this locus during T-DNA integration.

A comparison of predicted transmembrane (TM) helices (http://www.cbs.dtu.dk/services/TMHMM/) in MgAlg2 and ScAlg2 suggested for the former only a single TM domain occurring between amino acids 447–469, contrasting with the 4 predicted for ScAlg2 (Fig. 2D and Kampf *et al*., 2009). An alignment of MgAlg2 with Alg2 homologues identified in a range of eukaryotic sequenced genomes highlighted a clear separation of the filamentous fungal ascomycete sequences from those found in budding ascomycete yeasts and higher eukaryotes (Fig. S1A). Comparison of the predicted TM organization highlighted that the Alg2 homologues from all studied filamentous fungi share the same predicted single C-terminal TM domain found in MgAlg2 (Fig. S1B). This TM domain was not predicted for Alg2 proteins from higher eukaryotes including those from humans, plants, nematodes and fruit flies and was particularly notable in its absence from the Alg2 homologue of the opportunistic animal infecting fungus *Candida albicans*. In contrast, these organisms appear to possess Alg2 protein homologues, which have either only a single N-terminal TM domain or were not strongly predicted to possess TM domains (Fig. S1B).

MgAlg2 functionally complements the Saccharomyces cerevisiae *Alg2-1 temperature sensitive growth phenotype with and without its predicted transmembrane domain*

The Alg2-1 mutant of *S. cerevisiae* exhibits a temperature sensitive growth phenotype. This strain cannot grow at 34°C but grows well at 25°C (Huffaker and Robbins, 1982; Kampf *et al*., 2009). We tested whether *MgAlg2* was able to complement the temperature sensitive growth phenotype of the yeast Alg2-1 mutant by transforming with both a full-length *MgAlg2* sequence, and a truncated version encoding amino acids 1–446, thus omitting the C-terminal TM domain. Figure 2E highlights that both constructs were equally able to restore the growth of the yeast Alg2-1 strain at 34°C, in contrast to non-transformed strains and those transformed with the empty vector. This data demonstrates that *MgAlg2* encodes a functional homologue of *ScAlg2* and that the single C-terminal TM domain was not essential for its activity.

MgAlg2 function is essential for the fungal transition to hyphal growth and ability to cause Septoria Tritici Blotch disease

To confirm that the inability of the original 5-29H mutant to generate hyphae and cause STB disease of wheat leaves was caused by the loss of *MgAlg2* function, we performed independent targeted gene disruption of *MgAlg2* in the wild-type strain, and also complementation of the 5-29H mutant with the intact *MgAlg2* sequence along with its upstream (5′) and downstream (3′) genomic regions. Independent gene disruption mutants were obtained by *Agrobacterium*-mediated fungal transformation and correct gene targeting was confirmed by Southern blot analysis (Fig. S2). The results of plant infection assays with both the targeted disruption strains (ΔMgAlg2) and the 5-29H strain complemented with *MgAlg2* (5–29::MgAlg2) confirmed that the loss of *MgAlg2* function was responsible for the 5-29H phenotype (Fig. 3). Like the original 5-29H strain, the targeted ΔMgAlg2 mutant strains were unable to cause STB disease lesions or grow hyphally on TWA (Fig. 3). Importantly, the 5-29H::MgAlg2 complemented strain completely recovered both the ability to cause disease and grow hyphally on TWA (Fig. 3). *MgAlg2* was constitutively expressed during *in vitro* growth and throughout phases of plant infection spanning symptomless colonization (6 and 9 days post inoculation) and necrotrophic growth and sporulation (14 and 21 days post inoculation; Fig. S3). These data demonstrate that the

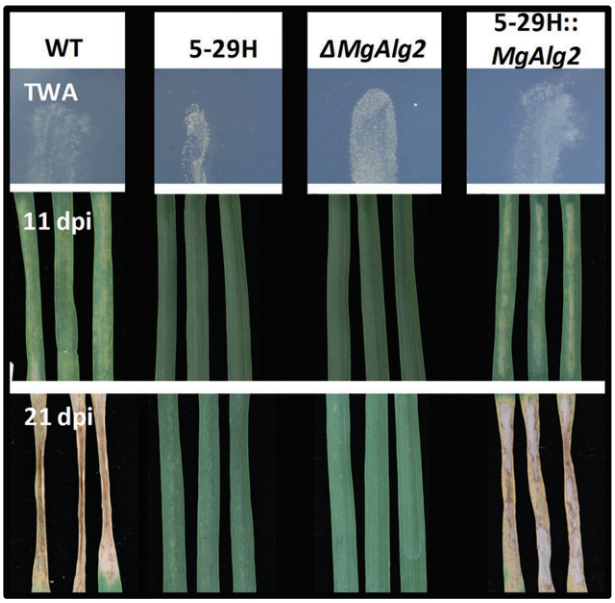

Fig. 3. Targeted deletion of *MgAlg2* and complementation of strain 5-29H with the intact *MgAlg2* gene confirms *MgAlg2* function in the regulation of hyphal growth and plant infection. Upper panels show each strain inoculated on tap water agar (TWA) plates to stimulate hyphal growth. Bottom two panels show three independently fungal inoculated wheat leaves for each of the four strains photographed at 11 and 21 days post inoculation. WT indicates the wild-type strain; 5-29H the mutant from the T-DNA mutagenesis screen; ΔMgAlg2 indicates an independently generated targeted deletion strain of *MgAlg2;* 5-29H::MgAlg2 indicates a strain produced by re-integration of the *MgAlg2* gene into the 5-29H mutant.

function of the constitutively expressed *MgAlg2* gene in the early steps of protein *N*-glycosylation is essential for the transition to hyphal growth under permissive conditions, including those presented by the surface of wheat leaves.

Spores of ΔMgAlg2 mutants exhibit hypersensitivity to Calcofluor white and are affected in temperature sensitive growth

A range of experiments were performed to determine whether loss of *MgAlg2* function caused macroscopic and/or structural changes in spores. *M. graminicola* spores are elongate and comprise 1–4 cells separated by septa. We measured median cell lengths defined as the distance between these septa. These measurements suggested there was a greater range of cell sizes produced by the ΔMgAlg2 mutant strains than the wild-type, although this was not attributable to a change in the number of cells present within a single spore. Overall, there was a tendency for a larger proportion of ΔMgAlg2 mutant cells being slightly shorter than their wild-type equivalents (Fig. S4). Transmission electron microscopy (TEM) on sections through both wild-type and ΔMgAlg2 spores revealed no obvious consistent macroscopic differences in overall cell structure, cell wall structure, or in septation or bud emergence (Fig. 4A). Despite these findings, both the original 5-29H mutant and the ΔMgAlg2 strains showed dramatically increased sensitivity to the cell wall perturbing agent Calcofluor white, indicating that cell wall integrity and strength was compromised by the loss of MgAlg2 function. In contrast, the complemented 5-29H::MgAlg2 strain did not exhibit this hypersensitivity (Fig. 4B). The ΔMgAlg2 mutant did not show increased sensitivity to growth on sorbitol, indicating that the cell wall defect was not caused by an increase in sensitivity to osmotic stress (Fig. 4C). Growth of the ΔMgAlg2 mutant was also reduced at 28°C, a temperature which stimulates hyphal (mycelial) growth of the wild-type strain (Fig. 4D). These data suggest that the cell wall strength of ΔMgAlg2 strains was affected by the loss of *MgAlg2* function.

*ΔMgAlg2 mutant cells possess abnormally hypo-*N*-glycosylated proteins with $(GlcNAc)_2Mann_1$ attachments*

We tested whether D-mannose-linked glycans were present on the surface of ΔMgAlg2 mutant strains through affinity binding of the FITC-labelled alpha-D-mannose/alpha-D-glucose-specific lectin Concanavalin-A (ConA) coupled with fluorescent microscopy. In terms of both the number of cells which bound ConA, and the relative intensity of staining, we were unable to detect consistent differences between ΔMgAlg2 mutant and wild-type cells (Fig. S5). This suggests that the ΔMgAlg2 mutant strain retains alpha-D-mannose/alpha-D-glucose on cell surface components. However, as ConA is able to bind to both *N*-linked and *O*-linked mannosylated proteins we needed to more directly assess the relative levels and structural identity of *N*-linked glycans in the ΔMgAlg2 mutant. To do this we used mass spectrometry to analyse the glycan chains released from total cellular proteins following treatment with Peptide-*N*-glycanase A (PNGase A). PNGase A is only able to release glycan chains which are *N*-linked to proteins and does not release those that are *O*-linked. *N*-linked glycans released from proteins of ΔMgAlg2 mutants were compared alongside those from the wild-type strain for the presence of intermediates leading to the formation of the core structure $(GlcNAc)_2Mann_9$, derived from processing of $(GlcNAc)_2Mann_9Glc_3$. This analysis revealed that the ΔMgAlg2 mutant still possessed some extended glycan structures attached to proteins including $(GlcNAc)_2Mann_9$ (m/z 2395.6; see Fig. 5). Although only semi-quantitative, it was clear however that the peak heights of the various glycans were much reduced for each of these moieties in the ΔMgAlg2 mutant when compared with the wild-type spores (Fig. 5).

Significantly, the most prevalent *N*-linked glycan released by PNGase A treatment from proteins in the ΔMgAlg2 mutant was $(GlcNAc)_2Mann_1$ (m/z 763.01; see Fig. 5) which derives from Dol-PP-$(GlcNAc)_2Mann_1$, the known substrate for Alg2 activity in the early steps of protein *N*-glycosylation (see Fig. 2A). The fact that this moiety was so prevalently released following PNGase A treatment suggests that it is more frequently transferred to proteins in the ΔMgAlg2 mutant. In contrast *N*-linked $(GlcNAc)_2Mann_1$ was much less frequently detected on proteins of the wild-type strain (Fig. 5). This suggests that although the ΔMgAlg2 mutant is able to extend (to some degree) the core structure for *N*-glycosylation $(GlcNAc)_2Mann_9Glc_3$, an abnormally high proportion of truncated *N*-linked glycans, in particular $(GlcNAc)_2Mann_1$, are found on proteins in these cells.

ΔMgAlg2 mutant spores exhibit changes in both the total proteome and glycoproteome

In order to better understand the physiological changes which might be associated with the hypo-*N*-glycosylation of cellular proteins in the ΔMgAlg2 mutant, we undertook some preliminary proteome-based analyses. Total protein extracts from both ΔMgAlg2 mutant and wild-type spores were analysed by SDS-PAGE and stained with either Coomassie blue or ProQ-Emerald, a fluorescent stain specific for glycosylated proteins. Both the total protein and glycoprotein staining profiles differed for extracts isolated, initially, from wild-type and 5-29H mutant spores (Fig. 6A). ProQ Emerald glycoprotein staining identified

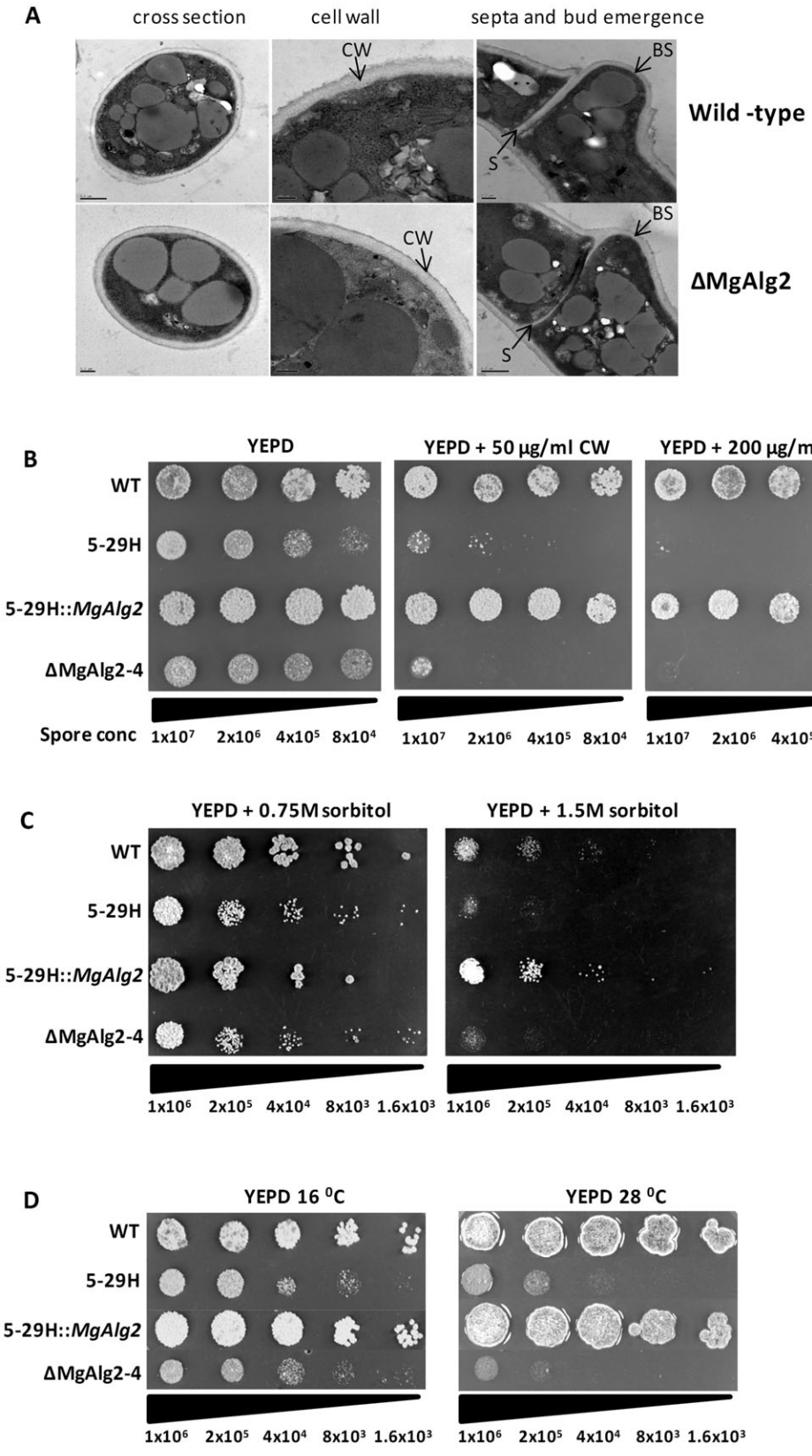
A
cross section
cell wall
septa and bud emergence
CW
BS
S
Wild -type
ΔMgAlg2
B
YEPD
YEPD + 50 µg/ml CW
YEPD + 200 µg/ml CW
WT
5-29H
5-29H::MgAlg2
ΔMgAlg2-4
Spore conc
1x10⁷ 2x10⁶ 4x10⁵ 8x10⁴
C
YEPD + 0.75M sorbitol
YEPD + 1.5M sorbitol
1x10⁶ 2x10⁵ 4x10⁴ 8x10³ 1.6x10³
D
YEPD 16 °C
YEPD 28 °C

Fig. 4. Examination of wild-type and ΔMgAlg2 mutant spore structure and sensitivity to stress.
A. Transmission electron microscopy (TEM) sections through wild-type and ΔMgAlg2 mutant spores. Keys to arrowheads; CW = cell wall, S = Septa; BS = Budding site.
B. Calcofluor white (cw) sensitivity assay. Serial dilutions of spores were applied to YEPD plates containing the indicated concentrations of cw and photographed after 6 days growth.
C. Osmotic stress (Sorbitol) sensitivity assay measured after 6 days.
D. Temperature sensitive growth on YEPD plates measured 6 days after inoculation at the indicated temperatures. The data highlight that the ΔMgAlg2 mutant spores exhibit hypersensitivity to Calcofluor white and a temperature sensitive growth defect.

numerous differences between the two strains. However the most obvious was an enhanced staining of two proteins with molecular weights (M_r) of approximately 75 and 77 kDa in the 5-29H mutant (Fig. 6A arrows). Staining for total protein also revealed a number of differences, in particular the appearance of two strong protein bands at M_r 72 and 60 kDa (Fig. 6A indicated with asterisks '*'). These glycoproteome and proteome changes were specific to the loss of MgAlg2 function as they were also detected in independently targeted ΔMgAlg2 mutant strains, but were not observed in the complemented 5-29H::MgAlg2 strain (Fig. 6B).

As we had previously shown that at least some *N*-linked glycans, albeit predominantly $(GlcNAc)_2Mann_1$, are still attached to proteins in the ΔMgAlg2 mutant we sought to determine whether any of the changes we detected in the glycoproteome were sensitive to pre-treatment of protein extracts with PNGase F, which acts to specifically remove *N*-glycans from proteins but, alike PNGase A, is unable to remove *O*-linked sugars. Figure 6C highlights that PNGaseF treatment did affect the overall glycoprotein staining of proteins from both the wild-type and ΔMgAlg2 mutant spores. However, the heavily stained 75 and 77 kDa glycoproteins were resistant to this treatment suggesting that they did not result from increased *N*-glycosylation in the ΔMgAlg2 mutant. The specificity of both the ProQ Emerald staining procedure and the PNGase F treatment was confirmed by the simultaneous

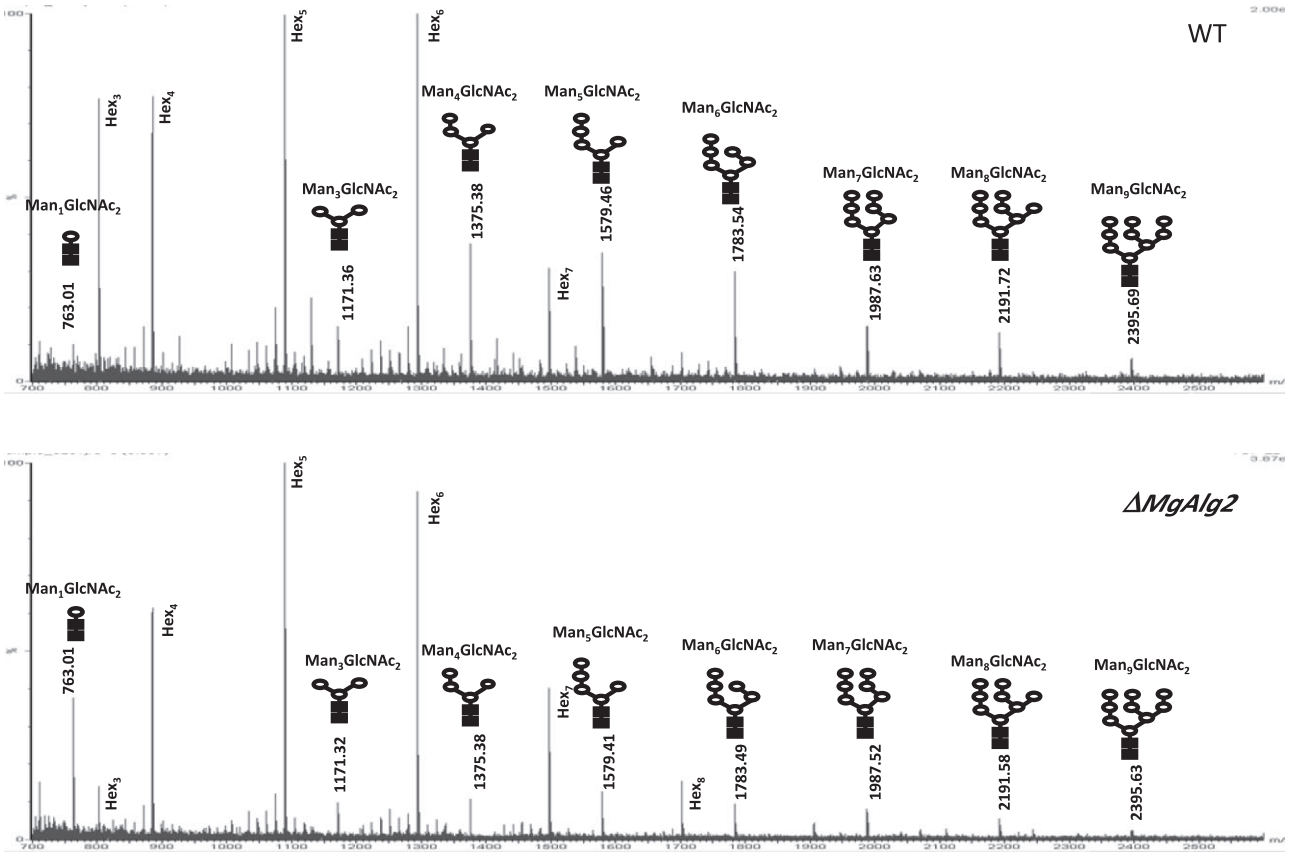

Fig. 5. Maldi-MS spectra of per-methylated *N*-glycans on proteins isolated from wild-type and ΔMgAlg2 mutant spores. PNGase A treatment was used to release the *N*-linked glycan from proteins. Spectra representing the $(GlcNAc)_2Mannose_x$ glycans are shown with the structures depicted above. Note the presence of a prominent peak for $(GlcNAc)_2Mannose_1$ (m/z 763.01) in the profile of the ΔMgAlg2 mutant which was much reduced in the wild-type fungus. The abbreviation Hex_x indicate peaks deriving from free hexoses also present in the samples.

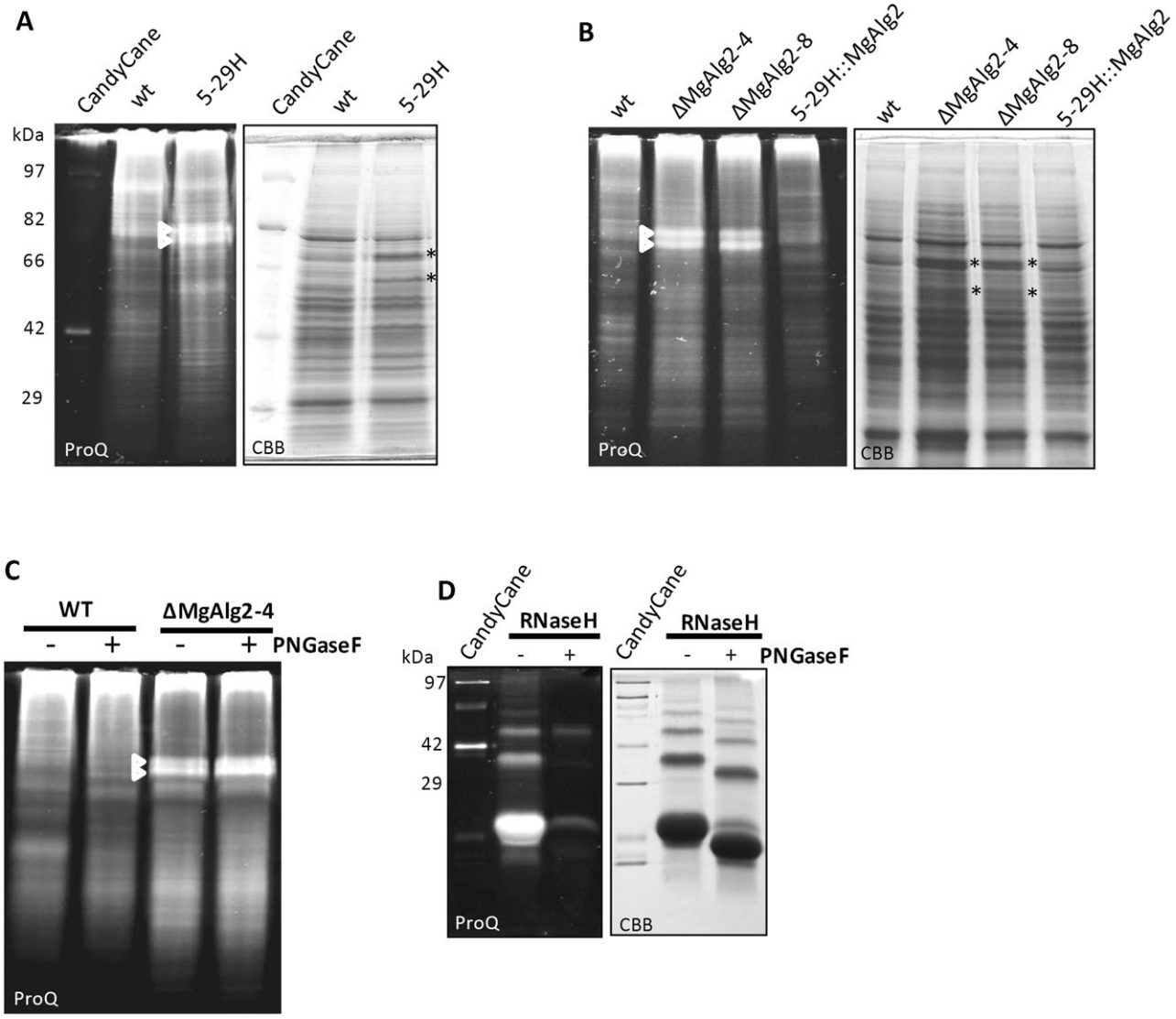

Fig. 6. Proteome and glycoproteome analysis of proteins extracted from wild-type and ΔMgAlg2 mutant spores.
A. Total protein extracts from wild-type or the 5-29H mutant, separated by SDS-PAGE and stained with ProQ-Emerald glycoprotein stain (ProQ) or Coomassie blue (CBB) along with CandyCane protein markers, which contain a 42 kDa control glycoprotein. Arrows indicate the presence of heavily stained glycoproteins in the original 5-29H mutant. Asterisks (*) highlight the presence of protein bands with increased staining intensity in the mutant.
B. Validation that the proteome changes derive from loss of MgAlg2 function. Experiments were performed as in (A) but included two independently generated ΔMgAlg2 mutants (-4 and –8) along with the complementation strain 5-29H::MgAlg2.
C. Proteins from the wild-type strain and ΔMgAlg2 mutants were de-*N*-glycosylated by pretreatment with PNGase F prior to electrophoresis and staining. Note the heavily stained glycoproteins in the MgAlg2 mutants were resistant to PNGase F treatment.
D. Controls for PNGase F treatment and ProQ-Emerald stain specificity using an *N*-glycosylated RNaseH protein standard.

treatment and staining of the *N*-glycosylated control protein Ribonuclease H (RNaseH) (Fig. 6D).

Genes implicated in cellular responses to mis-folded proteins are more highly expressed in spores of the ΔMgAlg2 mutant

The fact that ΔMgAlg2 mutants possess hypo-*N*-glycosylated proteins and also show differences in the total proteome and glycoproteome suggested that loss of *MgAlg2* might affect the correct folding, stability and localization of cellular proteins. In yeasts and mammals the accumulation of mis-folded proteins typically triggers increased expression of genes, which attempt to stabilize or increase the folding efficiency of proteins, including increased expression of various ER localized molecular chaperones. We analysed the fully sequenced *M. graminicola* genome to identify putative homologues of some of

the key marker genes, which respond to the accumulation of mis-folded proteins, and determined their expression levels in ΔMgAlg2 spores relative to wild-type spores. We studied the expression of homologues of *protein-O-mannosyltransferases (PMT) 1* and *2*, which catalyse the first reactions in protein *O*-mannosylation, and the molecular chaperones *KAR2* and an *Fkb1-like* peptidyl-prolyl *cis* isomerize (Table S1 provides the chromosomal locations and gene model Id codes for both the *M. graminicola* and corresponding *Saccharomyces cerevisiae* genes). Each of these genes exhibits increased expression in *S. cerevisiae* cells accumulating mis-folded proteins (Travers *et al*., 2000). As a comparison we measured the expression levels of a further two genes involved in the *N*-glycosylation pathway: *OST1*, which encodes a sub-unit of the protein oligosaccharide transferase complex, and *Alg11* encoding an alpha mannosyltransferase gene, which acts upon Dol-PP-$(GlcNac)_2Mann_3$ normally generated through the activity of Alg2 (details in Table S1). In contrast, there is no reported transcriptional activation of either *OST1* or *Alg11* in response to mis-folded proteins (Travers *et al*., 2000). The expression levels of all six genes were determined by real-time qPCR analysis on RNA isolated from spores undergoing budding growth in YEPD medium. All four genes anticipated to be upregulated in response to mis-folded proteins showed higher expression in ΔMgAlg2 mutants. This ranged from 3–10 fold greater levels than in the wild-type cells for individual genes (Fig. 7). In contrast, no significant change in transcript levels was detected for *MgOST1* and *MgAlg11*. These data suggest that loss of MgAlg2 function may result in the accumulation of mis-folded proteins, which are tolerated during yeast-like fungal growth, but which may prohibit the subsequent differentiation of hyphae.

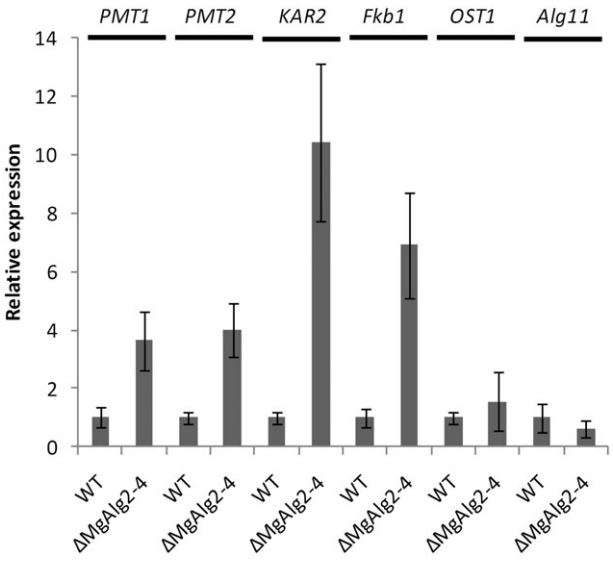

Fig. 7. Quantitative RT-PCR analysis on *M. graminicola* homologues of yeast genes responding to the accumulation of mis-folded proteins. The relative expression levels of *M. graminicola* homologues of *MgPMT1 (Protein O-mannosyltransferase 1)*, *MgPMT2 (Protein O-mannosyltransferase 2)*, *MgKAR2* (KARyogamy; ER-localized ATPase and chaperone) and *MgFkb1-like* (peptidyl-prolyl *cis-trans* isomerase) were determined in wild-type and ΔMgAlg2 mutant spores. The corresponding *Saccharomyces cerevisiae* genes all show elevated expression in response to the accumulation of mis-folded proteins. All four *M. graminicola* homologues of these genes were more highly expressed in ΔMgAlg2 mutant spores than in the wild-type spores. In contrast, no change in expression was detected for *MgOST1* and *MgAlg11* which are homologues of yeast genes, which do not respond to mis-folded proteins. Data are shown relative to the expression of the constitutive *M. graminicola beta tubulin* gene. The experiment was performed twice with similar results.

Discussion

Protein *N*-glycosylation is a ubiquitous post-translational modification conserved in eukaryotes and operates to confer the appropriate stability, functionality and localization of cellular proteins (Burda and Aebi, 1999; Lehle *et al*., 2006). Many proteins, which are secreted or cell wall localized, are frequently *N*-glycosylated in the ER prior to passage into the Golgi. This modification is particularly important for the correct folding of proteins (Helenius and Aebi, 2001). In fact, protein folding 'quality control' mechanisms exist in the ER in order to ensure, wherever possible, that only correctly folded functional proteins are produced and allowed to traverse through the Golgi apparatus. These quality control processes include activation of the Unfolded Protein Response (UPR), which is an ER to nucleus signalling pathway, which serves to increase the expression of genes whose function is to stabilize or assist in the folding of mis-folded proteins (Schroder *et al*., 2000; Travers *et al*., 2000; Mori, 2009). A second, and functionally coordinated mechanism, involves activation of the endoplasmic reticulum associated degradation pathway (ERAD) which serves to target terminally mis-folded proteins for destruction via the cytosolic proteosome network (Jakob *et al*., 1998; Ruddock and Molinari, 2006; Brodsky and Wojcikiewicz, 2009; Stolz and Wolf, 2010). Although the process of *N*-glycosylation has been most extensively studied in the yeast *S. cerevisiae*, defects in many steps in this pathway have been identified as the causes of many human congenital diseases (Freeze and Aebi, 2005; Lehle *et al*., 2006; Jaeken and Matthijs, 2007). For example, congenital disorder of glycosylation 1i (CDG-1i) is known to be caused by loss of function of the Alg2 homologue in humans (Thiel *et al*., 2003). These data highlight the global importance of correct and functional protein *N*-glycosylation for regulating cellular development.

During the course of a forwards genetic screen for genes, which play a role in virulence of the wheat leaf

infecting fungus *M. graminicola*, we identified *MgAlg2*, so named due to its homology to the *S. cerevisiae Alg2* gene. *ScAlg2* encodes an alpha 1,2- and 1,3-mannosyltransferase, which is responsible for the conversion of Dol-PP-$(GlcNAc)_2Mann_1$ through to Dol-PP-$(GlcNAc)_2Mann_3$ during the early ER associated steps of protein *N*-glycosylation (Jackson *et al*., 1993; Kampf *et al*., 2009). Interestingly, complete loss of *ScAlg2* function in yeast is lethal (Giaever *et al*., 2002), whereas loss of *MgAlg2* function was not. However, loss of *MgAlg2* function gave rise to a defect in a developmental process, which is normally essential for the ability of the fungus to infect wheat leaves. This defect was an inability of spores to extend hyphal filaments, which normally permit leaf penetration by the fungus through stomata. Although much of the data we have presented has identified various physiological and molecular differences between the spores of the wild-type and ΔMgAlg2 mutant strains, the most intriguing observation was that the typical budding yeast-like growth of *M. graminicola* spores, which occurs under nutrient rich and/or low temperature conditions, still occurred in ΔMgAlg2 mutant strains.

Protein glycosylation has been identified as an important process for the virulence of various fungal pathogens of animals. To date, most reports have described the importance of *O*-linked glycosylation (frequently *O*-mannosylation). For example, roles for PMTs have been well established to support both morphological transitions and host infection by *Cryptococcus neoformans* (Olson *et al*., 2007), *Candida albicans* (Timpel *et al*., 1998; 2000; Prill *et al*., 2005) and *Aspergillus fumigatus* (Mouyna *et al*., 2010). Other studies also implicated roles for *N*-glycosylation in virulence of *Candida albicans* through the analysis of mutants affected in the subsequent processing of high mannose-type glycans, following the initial transfer of the core oligosaccharide structure onto proteins (Bai *et al*., 2006; Bates *et al*., 2006). For plant infecting fungi, to date there are only two examples where defects in protein glycosylation have impacted upon pathogen development and virulence and these are both restricted to the basidiomycete fungus *Ustilago maydis*. *U. maydis* mutants lacking an ER associated glycan processing enzyme Glucosidase II were shown to grow normally *in vitro* but fail to effectively establish a host–pathogen interface with the plant (Schirawski *et al*., 2005), and the *O*-mannosyltransferase PMT4 was found to be essential for appressorium formation and penetration (Fernandez-Alvarez *et al*., 2009). The only functional analyses performed on putative fungal *Alg2* homologues have to date been restricted to *Rhizomucor pusillus* and *Neurospora crassa*. In these cases, despite some reported abnormalities in hyphal growth, no clear roles for aberrant protein *N*-glycosylation in regulating distinct morphological growth transitions were described (Yamazaki *et al*., 1998; Takeuchi *et al*., 1999; Resheat-Eini *et al*., 2008). Neither was detailed characterization of the potential impact of loss of gene function on cell physiology undertaken.

MgAlg2 was able to complement the temperature sensitive growth phenotype of ScAlg2-1, establishing its comparable biochemical activity. However, our analysis of predicted Alg2 proteins from a range of fungi, yeasts and higher eukaryotes identified a lack of strong consensus for the number and location of predicted TM spanning domains. For example, ScAlg2 is predicted to possess up to four regions, which might encode TM domains. However, recent data have demonstrated that many of these domains can be lost without affecting ScAlg2 function (Kampf *et al*., 2009). The authors concluded that the presence of a single N or C terminal TM domain alone is sufficient to localize the protein to the ER membrane and retain activity. However, a ScAlg2 construct lacking all four predicted TM domains was not tested in this study. MgAlg2, in contrast to ScAlg2, but in common to Alg2 homologues from all analysed ascomycete filamentous fungi, has only one predicted TM domain present at the extreme C-terminus of the protein. Moreover deletion of this domain did not impair the ability of MgAlg2 to complement the ScAlg2-1 temperature sensitivity phenotype, suggesting it was not essential for protein function. This suggests that the MgAlg2 protein is either tethered to the ER by other means, possesses another TM domain, which is not predicted by the TMHMM software, or exists free in the cytosol of the cell. The fact that the early steps in the build-up of the core glycan structure involving Alg2 homologues occur on the cytosolic side of the ER membrane supports the possibility that a non-membrane attached enzyme might be able to carry out this function. However, due to the fact that ScAlg2 has been experimentally determined to be membrane associated (Kampf *et al*., 2009), it is possible that MgAlg2 might still be tethered to the ER membrane by a mechanism, which does not involve a recognizable TM domain.

Phenotypic characterization of the ΔMgAlg2 mutant highlighted a hypersensitivity to the cell wall destabilizing agent Calcofluor white. Despite the fact we were unable to detect consistent gross macroscopic changes in cell wall structure between wild-type and ΔMgAlg2 mutants via TEM, these data nonetheless suggest that the cell walls in the mutant strain lack the structural strength of wild-type spores. This was not attributable to an increase in osmosensitivity and is thus more likely to result from altered cell wall composition. Studies on protein *N*-glycosylation mutants in *S. cerevisiae* have suggested that defects in cell wall strength may arise from alterations in the chemical composition of the glucans normally present in this structure. One hypothesis put forward to explain this link was

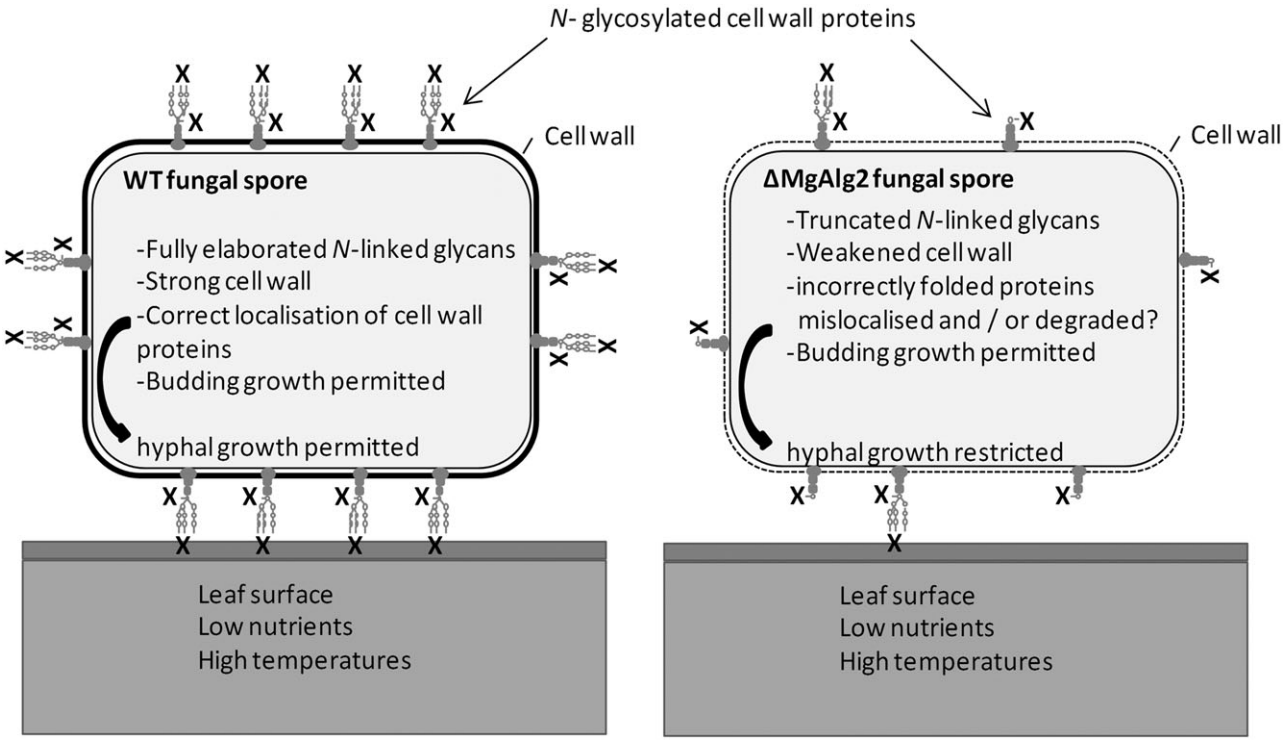

Fig. 8. Summary model for the possible impact of loss of *MgAlg2* function on infection related growth transitions of *M. graminicola*. The possible events and/or defects, which might contribute to the inability of ΔMgAlg2 mutant fungal spores to differentiate hyphae, are highlighted. 'X' represents any of the numerous as yet undefined modifications, which can be normally found on extended *N*-linked glycan chains. A wild-type fungal spore is indicated on the left with the ΔMgAlg2 mutant to the right.

that particular proteins normally subject to *N*-glycosylation were not correctly processed and localized in the *N*-glycosylation mutant strain (Chavan *et al*., 2003). Our analysis of the *N*-linked glycans released from total cell proteins of ΔMgAlg2 mutants following PNGase A treatment highlighted that many proteins were hypo-*N*-glycosylated, frequently possessing a $(GlcNAc)_2Mann_1$ attachment. This is in contrast to the core structure most frequently transferred in eukaryotes; $(GlcNAc)_2Mann_9Glc_3$, prior to its subsequent processing. The fact that some extended *N*-glycans were still found attached to proteins, suggests that there may be some level of functional overlap of MgAlg2 with other protein(s) possessing an *N*-mannosyltransferase activity. This protein(s) remains to be identified, although we were able to detect homologues of various other *S. cereviseae Alg* genes in the *M. graminicola* genome (Table S3). However, the data provided highlights that *M. graminicola* is able to transfer truncated or precurser dolichol-linked glycans onto proteins and supports what has been reported for *N*-glycosylation mutants in *S. cerevisiae* (Huffaker and Robbins, 1983; Verostek *et al*., 1991; 1993) and the *Rhizomucor pusillus* fungus (Murakami *et al*., 1994; Takeuchi *et al*., 1999). The impact of hypo-*N*-glycosylation on the functions and localization of specific *M. graminicola* proteins remains to be determined, but it is conceivable that many might be mis-folded and perhaps subjected to quality control mechanisms, which could preclude their function in stabilizing the fungal cell wall.

The data provided support the idea that protein mis-folding and activation of quality control mechanisms in the spores of ΔMgAlg2 mutants may play roles in prohibiting the switch to hyphal growth (Fig. 8). For example, preliminary investigation of the glycoproteome, as revealed by ProQ Emerald staining, identified two heavily stained protein bands in the mutant spores which were resistant to PNGaseF treatment. This suggested that they were not extensively or aberrantly *N*-glycosylated. It is therefore possible that the two highly stained proteins arise from enhanced *O*-glycosylation. This has been shown to occur in yeasts when particular types of protein folding stresses are imposed upon the ER, which would otherwise threaten the essential functions of particular proteins. In this situation these proteins can become hyper *O*-glycosylated as a consequence of enhanced *O*-mannosylation in order to prevent their destruction by ERAD (Harty *et al*., 2001; Nakatsukasa *et al*., 2004). That this might be true for some of the novel heavily glycan-stained, but PNGaseF-resistant, protein species in the ΔMgAlg2 mutants, is supported by the fact that homo-

logues of the first two key enzymes in the pathway of protein *O*-mannosylation, *PMT 1* and *2* also had increased expression in the ΔMgAlg2 mutant spores. Such increases in expression of *PMT* genes are also typical of yeast cells undergoing ER stress in response to mis-folded proteins (Travers *et al*., 2000). Further support for the accumulation of mis-folded proteins in ΔMgAlg2 mutants comes from the elevated expression of homologues of ER-localized molecular chaperones, which are typically regarded as marker genes for the activation of the un-folded protein response in *S. cerevisiae*, including *MgKAR2* and *Fkb1*-like genes (Schroder *et al*., 2000; Travers *et al*., 2000).

The availability of stable genetic deletion strains of *MgAlg2* opens up new research possibilities for the future. First, this material may be useful for the identification of cell surface/cell wall proteins which normally provide the rigidity and strength and may facilitate the transition to hyphal growth. It is conceivable that these proteins may in fact be *N*-linked glycoproteins, which fail to fold properly due to hypo-*N*-glycosylation and do not become incorporated into cell walls. Second, the preliminary proteome and gene expression analysis suggest that elements of the quality control apparatus are activated in the ΔMgAlg2 mutant spores. It is interesting to note that these mechanisms, and in particular the unfolded protein response, have recently been shown to regulate pathogenic development of the human opportunistic fungus *Aspergillus fumigatus* (Richie *et al*., 2009). We have identified numerous homologues of *Alg* genes, which might function downstream of *MgAlg2* leading to the synthesis of the core glycan structure in the *M. graminicola* genome, opening up the possibility of generating mutant strains for each of these genes. This approach, in combination with analysing homologues of key regulators of the protein folding quality control machinery, may elucidate mechanisms which control growth transitions, which are ultimately critical for the plant pathogenic lifestyle of *M. graminicola*. This may lead to the identification of novel fungal proteins which could be used as targets for future control of STB disease of wheat.

Experimental procedures

Plant and fungal material

The fully sequenced *M. graminicola* isolate IPO323 was used in all experiments (http://genome.jgi-psf.org/Mycgr3/Mycgr3.home.html). Fungal spores were harvested from 7-day-old cultures growing (budding) on YEPD plates (Oxoid, Hampshire, UK) at 15°C. For analysis of the ability of strains to form hyphae *in vitro*, spores collected from YEPD plates were streaked onto sterile tap water agar plates (1% agar) and visualized after 10 days. For analysing the sensitivity of spores to Calcofluor white or sorbitol, sterile filtered stock solutions were dissolved in YEPD agar. Serial dilutions of spores retrieved from YEPD plates were then applied as 5 μl droplets in sterile distilled water. Photographs of the relative colony densities were taken after 6–10 days incubation.

For plant infection the second leaves of 17-day-old wheat seedlings of cultivar Riband were attached, adaxial side up, to Perspex sheets using double sided tape. The inoculation procedure was as described previously (Keon *et al*., 2007). The leaves were inoculated evenly with fungal spores at a density of 1×10^7 cells ml^{-1} (or serial dilutions of) in water containing 0.1 % v/v Tween 20. Following 72 h incubation at 100% relative humidity, inoculated plants were incubated at 16°C with a 16 h light period at 88% relative humidity for up to 40 days. Leaf tissues were excised at various time points after inoculation and/or infiltration and stored at –80°C for RNA isolation.

Fungal and eukaryotic genome sequence resources used

The following genome sequence repositories were used to identify Alg2 homologues from a range of eukaryotes using ScAlg2 in Blastp analysis. ScAlg2 protein sequence (YGL065C) was obtained from http://www.yeastgenome.org/. To identify the listed fungal homologues of ScAlg2 the BROAD (http://www.broadinstitute.org/scientific-community/science/projects/fungal-genome-initiative/fungal-genome-initiative) and JGI (http://genome.jgi-psf.org/) databases were used. The following databases were used to identify Alg2 homologues from non-fungal eukaryotes; *Homo sapiens* (http://genome.ucsc.edu/cgi-bin/hgGateway?org=Human&db=hg19&hgsid=189726861); *Caenorhabditis elegans* (http://www.wormbase.org/); *Drosophila melanogaster* (http://genome.ucsc.edu/cgi-bin/hgGateway?db=dm2); *Arabidopsis thaliana* (http://www.arabidopsis.org/); *Dictyostelium discoideum* (http://dictybase.org/). Protein sequences were aligned using ClustalW (http://www.ch.embnet.org/software/ClustalW.html) and Phylip (http://www.phylip.com/). Protein TM domain prediction was done using TMHMM (http://www.cbs.dtu.dk/services/TMHMM/).

Generation of T-DNA insertional mutant 5-29H and gene deletion and complementation strains for MgAlg2

A library of T-DNA insertion mutants was generated in isolate IPO323 by *Agrobacterium*–mediated transformation using *Agrobacterium* strain Agl-1 harbouring the vector pCHYG, which provides resistance to Hygromycin B (Motteram *et al*., 2009). This led to the identification of mutant 5-29H. For targeted disruption of the *MgAlg2* gene two regions (flanks) of approximately 750 bp of fungal genomic DNA were amplified by PCR. Flank1 was then cloned into vector pCHYG using SacI and KpnI and Flank 2 using PstI and HindIII. The resulting plasmid was then used to transform Agl-1 via the freeze-thaw method (An *et al*., 1988). Strains harbouring the plasmid were then used for fungal transformation. For targeted gene disruption we used a modified ΔKu70 strain of IPO323 (Bowler *et al*., 2010). To generate the complementation strain 5-29H::MgAlg2 the entire open reading frame of *MgAlg2* plus

upstream and downstream sequences was amplified by PCR on genomic DNA. The amplicon was cloned using SacI and KpnI into vector pCGEN for fungal transformation of strain 5-29H and selection using 100 μg ml^{-1} Geneticin. pCGEN was generated by replacing the *TrpC–Hph* region in vector PCHYG with the *Cochliobolus heterostrophus Pgpd1-Gen* construct excised from vector pSK666 (provided by Martin Urban, Rothamsted Research). *Agrobacterium*-mediated transformation of *M. graminicola* was performed as previously described (Motteram *et al*., 2009; Zwiers & de Waard, 2001). For targeted mutants, homologous recombination was initially confirmed by PCR on genomic DNA and then subsequently by Southern analysis. All nucleotide primer sequences are provided in Table S2.

Isolation of fungal genomic DNA

DNA for use in PCR screening was extracted from 5–10 mg of freeze dried and ground fungal spores using Fastprep FP120 with 350 μl of TEN buffer (500 mM NaCl, 400 mM Tris-HCL, 50 mM EDTA, pH 8.0), 1% beta-mercaptoethanol, 5 mM 1,10-phenanthroline and 2% (w/v) polyvinylpyrrolidone K30 following an established protocol (Motteram *et al*., 2009). All DNA samples were quantified using a Thermo Scientific NanoDrop 1000 Spectrophotometer and diluted to 10 ng μl^{-1} for use in PCR. Genomic DNA for use in Southern blotting was extracted from 40 mg freeze dried and ground (Fastprep FP120) mycelium. Nucleic acid extraction was achieved by disruption in 800 μl of Lee and Taylor lysis buffer (Lee and Taylor, 1990) and incubation at 65°C for 60 min as per previous published protocol (Motteram *et al*., 2009). For Southern hybridization 7 μg of DNA was digested with XhoI prior to electrophoresis.

Identification of T-DNA insertion sites by thermal asymmetric interlaced (TAIL) PCR

TAIL PCR was carried out on fungal genomic DNA isolated from the 5-29H mutant according to the method of Liu *et al*. (1995) using degenerate primers AD 1, 2, or 3 and Left border primers LB1, LB2 and LB3 (Table S1). PCR products were purified (Qiagen PCR purification kit) and sequenced using primer LB3 (Eurofins MWG). Resulting sequences were used in a Blastn search against the *M. graminicola* genome sequence (http://genome.jgi-psf.org/cgi-bin/searchGM?db=Mycgr3).

Southern blot analysis

Seven micrograms of digested fungal genomic DNA was subjected to alkaline Southern blotting via capillary transfer onto nylon membranes (Hybond N + Amersham Pharmacia). An 185 bp DNA probe was amplified by PCR. Probe labelling was achieved with ^{32}Palpha-dCTP (3000 Ci mmol^{-1}, NEN Ltd) using the Amersham Pharmacia Rediprime random prime labelling kit. Prehybridization and probe hybridization was performed at 65°C according to the method of Church and Gilbert (Church & Gilbert, 1984). Blots were washed at 65°C twice with 2× SSC/0.1% SDS and once with 0.5× SSC/0.1% SDS. Filters were subsequently developed by phosphorimaging (Typhoon 8600, Molecular Dynamics).

RNA isolation and real-time RT-PCR with Sybr-Green detection

Total RNA was isolated from freeze-dried, filtered fungal material collected during log phase growth in liquid (YEPD) cultures or from infected leaf tissues using the TRIZOL procedure (Invitrogen). Total RNA was used for all real-time RT-PCR analyses. First-stranded cDNA was synthesized from total RNA using the SuperScript III First_Strand Synthesis System for RT-PCR (Invitrogen). A 5 μg aliquot of total RNA primed with oligo(dT)$_{20}$ was used in a 20 μl reaction, following the suppliers instructions. The resulting cDNA was analysed using a QuantiTect SYBR Green PCR Kit (QIAGEN), following the suppliers' instruction. A 0.5 μl aliquot of cDNA was used in a 20 μl PCR reaction, with an annealing temperature of 60°C. Primers were added at a final concentration of 0.25 μM. The PCR reactions were run and analysed using an ABI 7500 Real Time PCR System. For expression normalization the beta-tubulin genes were used for *M. graminicola* (Keon *et al*., 2005; 2007; Rudd *et al*., 2010).

Yeast complementation and temperature sensitivity experiments

Saccharomyces cerevisiae mutant Alg2-1 (genotype MAT alpha ura3-52 ade2-101) was made competent using the Invitrogen Easycomp system following the manufacturer's guidelines. Either full-length or truncated *MgAlg2* sequences were amplified from cDNA using primers containing restriction sites KpnI and SacI. Digested DNA was ligated into vector pYES2 (Invitrogen) and transformed into the Alg2-1 mutant following standard protocols. Transformants were selected for growth on medium lacking uracil and then incubated at either 25°C or 36°C for 5 days. Plates were then photographed to record yeast growth.

Protein and glycoprotein analysis

Total cellular proteins were extracted from freeze dried fungal spores in 50 mM Tris-HCl, 1 mM DTT, 1 μg ml^{-1} Leupeptin and Aprotinin. For analysis of *N*-linked glycans protein extracts were dialysed overnight against sterile distilled water. For SDS-PAGE and glycoprotein staining, 50 μg of protein was loaded per lane. Gels were first stained with the fluorescent stain Pro-Q Emerald (Invitrogen) according to the supplier's protocol with signals detected by imaging on a UV box. Gels were then subsequently stained for total protein with Coomassie blue R250. For deglycosylation of *N*-glycoproteins we used the Glycoprofile II enzymatic *N*-deglycosylation kit (Sigma Aldrich) containing PNGaseF and the RNaseH glycoprotein standard, prior to gel electrophoresis.

Mass spectrometry analysis on N*-linked glycans*

Fungal proteins were adjusted in water to a concentration of 100 μg ml^{-1}. To 100 μl of fungal extract was added 28 μl of a

1 mg ml^{-1} pepsin solution [in 5% (v/v) formic acid] mixed and incubated at 37°C for 24 h. The pepsin was inactivated by heating to 100°C for 5 min, and the resulting glycopeptides were then lyophilized. To release the *N*-glycans the glycopeptides dissolved in 50 mM ammonium acetate pH 5 and 4 μl of PNGase A added and incubated at 37°C for 16 h. The sample was then freeze-dried. Glycans were then purified by passage through a Sep-Pak C18 cartridge. Briefly, the cartridge was wetted with 100% methanol and then equilibrated with 5% (v/v) acetic acid. The sample, in 0.5 ml of 5% (v/v) acetic acid, was loaded and eluted with 5% (v/v) acetic acid, leaving non-polar peptides behind. The eluted glycans were then lyophilized and passed through Dowex 50WX8-100 resin. The Dowex resin was washed repeatedly with 4 M HCl, and then with water until the pH had returned to that of the water. The Dowex was then washed three times in 5% (v/v) acetic acid and packed into a Pasteur pipette, with glass wool as a frit. The lyophilized sample was dissolved in 100 μl 5% (v/v) acetic acid and eluted with the same, leaving behind any salt and polar peptides. The eluted glycans were lyophilized.

Per-methylation of lyophilized glycan samples was performed according to the method of Dell *et al.* (1994). The derivatized glycans were then redissolved in 200 μl of 35% (v/v) acetonitrile and passed through another Sep-Pak C18 cartridge. The glycans were eluted with 50% (v/v) acetonitrile and freeze-dried. The *per*-methylated glycan samples were dissolved in 30 μl of 10 mg ml^{-1} 2,5-dihydroxybenzoic acid (DHB) in 50% (v/v) methanol. One microlitre was spotted in triplicate on the MALDI target and allowed to air-dry.

MALDI-ToF-MS was carried out using a Micromass M@LDI-LR mass spectrometer (Waters, Manchester, UK) using a standard peptide mass fingerprinting method and mass acquisition between 700 and 3500 m/z. The laser firing rate was 5 Hz, 40 random aims per spot, 10 shots per spectrum, 10 spectra per scan, 10 scans combined, 10% adaptive background subtracted, smoothed (Savitzky-Golay) and centroided to obtain MS spectra shown. The MALDI-MS was tuned to 10 000 FWHM (full width at half height) and calibrated with a tryptic digest of ADH following the manufacturer's instructions. At least 6 peaks were matched out of 12 with mean residue values of $10^{-3} \pm 0.007$ or better. Glycan molecular ions $[M+Na]^+$ were assigned.

Fluorescent microscopy

Conidia were fixed in 4 % paraformaldehyde in 0.05 M phosphate buffer for 30 min. The samples were then washed three times in buffer followed by incubation in 20 μg ml^{-1} FITC-labelled concanavalin A (Fluka supplied by Sigma-Aldrich, Dorset, England) for 2 h. The samples were then rinsed in buffer and imaged with a FITC filter set (excitation: 450–490 nm, emission: LP 515 nm) using a Zeiss Axiophot microscope (Carl Zeiss, Jena, Germany) and a QImaging Retiga Exi CCD camera (QImaging, Canada). Cell lengths described as the distance between septa in multi cell spores were measured after Calcofluor white M2R staining and imaging using the microscope above using MetaMorph v. 7.5 image analysis software.

Preparation of samples for examination using the JSM 6700 FEG Scanning Electron Microscope (Jeol UK)

Electron microscopy examination was used to study the germination, morphology of hyphal growth and possible penetration of the pathogen on host leaves. Sections of leaf tissue (5 mm × 5 mm) were cut from the centre of the inoculation zone using a sterile razor blade. This was quickly mounted on a cryo stub using OCT compound (Sakura Finetek, Europe NL) and plunge frozen in pre slushed LN_2. The sample was then transferred under vacuum to the Gatan Alto 2500 cryo prep chamber (Gatan UK) where the temperature was maintained at –180°C. The sample was etched to remove contaminating ice and coated with AuPd. It was then transferred to the microscope (JSM 6700 FEGSEM; Jeol UK) for examination with the microscope stage temperature maintained at –150°C throughout. Images were recorded and saved using the on-board system and software.

Preparation of samples for examination using the Jeol 2011 FasTEM Transmission Electron Microscope (Jeol UK)

Spores were scraped from the surface of each culture plate using a sterile blade, transferred to an Eppendorf and gently agitated for 10 min in 1 ml of fixative (4% paraformaldehyde, 0.5% glutaraldehyde in 0.05 M phosphate buffer pH 7.2). They were removed from the agitator and placed in the fridge (4°C) over night. Samples were washed in 0.05 M phosphate buffer three times then 1 ml of 1% osmium tetroxide in 0.05 M phosphate buffer was added to the pellet and gently agitated. Tubes were double sealed and placed in the fridge (4°C) for 2 h. Samples were washed in phosphate buffer three times with 10 min intervals before dehydrating through a graded acetone series of 30%, 50%, 70%, 90% and 100% with 30 min intervals. The samples were infiltrated with Spurr's resin starting with 30% of resin : acetone, 50%, 70% 100%. After two changes in 100% resin the samples were placed in Beem capsules (TAAB Laboratories Equipment UK) or 0.5 μl Eppendorf tubes and polymerized at 60°C for 12 h. Ultrathin sections 60–80 nm thick were cut with a glass knife from these blocks using a Leica EM UC6 ultramicrotome (Leica Microsystems UK), stained with uranyl acetate and lead citrate and examined in the transmission electron microscope JSM 2011 FasTEM (Jeol UK). Images were captured on a Ultrascan 1000 CCD digital camera (Gatan UK) using Gatan Digital Micrograph software.

Acknowledgements

We would like to thank Judith Bowler and Mike Csukai (Syngenta, Jealotts Hill, UK) for providing the ΔKu70 modified strain of fungal isolate IPO323. We also thank Professor Ludwig Lehle (University of Regensberg Germany) for the provision of the yeast Alg2-1 strain and Professor John Lucas for critically reading the manuscript. Rothamsted Research receives grant aided support from the Biotechnology and Biological Sciences Research Council (BBSRC) of the UK.

References

An, G., Ebert, P.R., Mitra, A., and Ha, S.B. (1988) Binary vectors. In *Plant Molecular Biology Manual A3*. Gelvin, S.B., and Schilperroort, R.A. (eds). Dordrecht: Kluwer Academic Press, pp. 1–19.

Bai, C., Xu, X.L., Chan, F.Y., Lee, R.T.H., and Wang, Y. (2006) MNN5 encodes an iron-regulated alpha-1,2-mannosyltransferase important for protein glycosylation, cell wall integrity, morphogenesis and virulence in *Candida albicans*. *Eukaryot Cell* **5:** 238–247.

Bates, S., Hughes, H.B., Munro, C.A., Thomas, W.P.H., MacCallum, D.M., Bertram, G., *et al*. (2006) Outer chain *N*-glycans are required for cell wall integrity and virulence of *Candida albicans*. *J Biol Chem* **281:** 90–98.

Borges-Walmsley, M.I., Chen, D.L., Shu, X.H., and Walmsley, A.R. (2002) The pathobiology of *Paracoccidioides brasiliensis*. *Trends Microbiol* **10:** 80–87.

Bowler, J., Scott, E., Tailor, R., Scalliet, G., Ray, J., and Csukai, M. (2010) New capabilities for *Mycosphaerella graminicola* research. *Mol Plant Pathol* **11:** 691–704.

Brodsky, J.L., and Wojcikiewicz, R.J.H. (2009) Substrate-specific mediators of ER associated degradation (ERAD). *Curr Opin Cell Biol* **21:** 516–521.

Burda, P., and Aebi, M. (1999) The dolichol pathway of *N*-linked glycosylation. *Biochim Biophys Acta-Gen Subj* **1426:** 239–257.

Chavan, M., Suzuki, T., Rekowicz, M., and Lennarz, W. (2003) Genetic, biochemical, and morphological evidence for the involvement of *N*-glycosylation in biosynthesis of the cell wall beta 1,6-glucan of *Saccharomyces cerevisiae*. *Proc Natl Acad Sci USA* **100:** 15381–15386.

Church, G.M., and Gilbert, W. (1984) Genomic sequencing. *Proc Natl Acad Sci USA* **81:** 1991–1995.

Dell, A., Reason, A.J., Khoo, K.H., Panico, M., McDowell, R.A., and Morris, H.R. (1994) Mass-spectrometry of carbohydrate-containing bioplymers. *Guide Tech Glycobiol* **230:** 108–132.

Deshpande, N., Wilkins, M.R., Packer, N., and Nevalainen, H. (2008) Protein glycosylation pathways in filamentous fungi. *Glycobiology* **18:** 626–637.

Fernandez-Alvarez, A., Elias-Villalobos, A., and Ibeas, J.I. (2009) The O-mannosyltransferase PMT4 is essential for normal appressorium formation and penetration in *Ustilago maydis*. *Plant Cell* **21:** 3397–3412.

Freeze, H.H., and Aebi, M. (2005) Altered glycan structures: the molecular basis of congenital disorders of glycosylation. *Curr Opin Struct Biol* **15:** 490–498.

Giaever, G., Chu, A.M., Ni, L., Connelly, C., Riles, L., Veronneau, S., *et al*. (2002) Functional profiling of the *Saccharomyces cerevisiae* genome. *Nature* **418:** 387–391.

Harty, C., Strahl, S., and Romisch, K. (2001) O-mannosylation protects mutant alpha-factor precursor from endoplasmic reticulum-associated degradation. *Mol Biol Cell* **12:** 1093–1101.

Helenius, A., and Aebi, M. (2001) Intracellular functions of *N*-linked glycans. *Science* **291:** 2364–2369.

Huffaker, T.C., and Robbins, P.W. (1982) Temperature sensitive yeast mutants deficient in asparagine-linked glycosylation. *J Biol Chem* **257:** 3203–3210.

Huffaker, T.C., and Robbins, P.W. (1983) Yeast mutants deficient in protein glycosylation. *Proc Natl Acad Sci USA* **80:** 7466–7470.

Jackson, B.J., Kukuruzinska, M.A., and Robbins, P. (1993) Biosynthesis of Asparagine linked oligosaccharides in Saccharomyces cerevisiae- The Alg2 mutation. *Glycobiology* **3:** 357–364.

Jaeken, J., and Matthijs, G. (2007) Congenital disorders of glycosylation: a rapidly expanding disease family. *Annu Rev Genomics Hum Genet* **8:** 261–278.

Jakob, C.A., Burda, P., Roth, J., and Aebi, M. (1998) Degradation of misfolded endoplasmic reticulum glycoproteins in *Saccharomyces cerevisiae* is determined by a specific oligosaccharide structure. *J Cell Biol* **142:** 1223–1233.

Kamper, J., Kahmann, R., Bolker, M., Ma, L.J., Brefort, T., Saville, B.J., *et al*. (2006) Insights from the genome of the biotrophic fungal plant pathogen *Ustilago maydis*. *Nature* **444:** 97–101.

Kampf, M., Absmanner, B., Schwarz, M., and Lehle, L. (2009) Biochemical characterization and membrane topology of Alg2 from *Saccharomyces cerevisiae* as a bifunctional alpha 1,3-and 1,6-mannosyltransferase involved in lipid-linked oligosaccharide biosynthesis. *J Biol Chem* **284:** 11900–11912.

Kema, G.H.J., Yu, D.Z., Rijkenberg, F.H.J., Shaw, M.W., and Baayen, R.P. (1996) Histology of the pathogenesis of *Mycosphaerella graminicola* in wheat. *Phytopathology* **86:** 777–786.

Keon, J., Rudd, J.J., Antoniw, J., Skinner, W., Hargreaves, J., and Hammond-Kosack, K.E. (2005) Metabolic and stress adaptation by *Mycosphaerella graminicola* during sporulation in its host revealed through microarray transcription profiling. *Mol Plant Pathol* **6:** 527–540.

Keon, J., Antoniw, J., Carzaniga, R., Deller, S., Ward, J.L., Baker, J.M., *et al*. (2007) Transcriptional adaptation of *Mycosphaerella graminicola* to programmed cell death of its susceptible wheat host. *Mol Plant Microbe Interact* **20:** 178–193.

Klein, B.S., and Tebbets, B. (2007) Dimorphism and virulence in fungi. *Curr Opin Microbiol* **10:** 314–319.

Klosterman, S.J., Perlin, M.H., Garcia-Pedrajas, M., Covert, S.F., and Gold, S.E. (2007) Genetics of morphogenesis and pathogenic development of *Ustilago maydis*. *Adv Genet* **57:** 1–47.

Kukuruzinska, M.A., and Lennon, K. (1994) Growth-related coordination of the early *N*-glycosylation genes in yeast. *Glycobiology* **4:** 437–443.

Lee, S.B., and Taylor, J.W. (1990) Isolation of DNA from fungal mycelia and single spores. In *PCR Protocols. A Guide to Methods and Applications*. Innis, M.A., Gelfand, D.H., Sninsky, J.J., and White, T.J. (eds). San Diego, CA: Academic Press, pp. 282–287.

Lehle, L., Strahl, S., and Tanner, W. (2006) Protein glycosylation, conserved from yeast to man: a model organism helps elucidate congenital human diseases. *Angew Chem Int Ed* **45:** 6802–6818.

Lengeler, K.B., Davidson, R.C., D'Souza, C., Harashima, T., Shen, W.C., Wang, P., *et al*. (2000) Signal transduction cascades regulating fungal development and virulence. *Microbiol Mol Biol Rev* **64:** 746–785.

Lennon, K., Bird, A., and Kukuruzinska, M.A. (1997) Deregulation of the first N-glycosylation gene, ALG7, perturbs the

expression of G1 cyclins and cell cycle arrest in *Saccharomyces cerevisiae*. *Biochem Biophys Res Commun* **237:** 562–565.

Liu, Y.G., Mitsukawa, N., Oosumi, T., and Whittier, R.F. (1995) Efficient isolation and mapping of *Arabidopsis thaliana* T-DNA insert junctions by thermal asymmetric interlaced PCR. *Plant J* **8:** 457–463.

Lommel, M., and Strahl, S. (2009) Protein O-mannosylation: Conserved from bacteria to humans. *Glycobiology* **19:** 816–828.

Mehrabi, R., Zwiers, L.H., de Waard, M.A., and Kema, G.H.J. (2006) MgHog1 regulates dimorphism and pathogenicity in the fungal wheat pathogen *Mycosphaerella graminicola*. *Mol Plant Microbe Interact* **19:** 1262–1269.

Mori, K. (2009) Signalling pathways in the unfolded protein response: development from Yeast to mammals. *J Biochem* **146:** 743–750.

Motteram, J., Kufner, I., Deller, S., Brunner, F., Hammond-Kosack, K.E., Nurnberger, T., and Rudd, J.J. (2009) Molecular characterization and functional analysis of MgNLP, the sole NPP1 domain-containing protein, from the fungal wheat leaf pathogen *Mycosphaerella graminicola*. *Mol Plant Microbe Interact* **22:** 790–799.

Mouyna, I., Kniemeyer, O., Jank, T., Loussert, C., Mellado, E., Aimanianda, V., *et al*. (2010) Members of protein O-mannosyltransferase family in *Aspergillus fumigatus* differentially affect growth, morphogenesis and viability. *Mol Microbiol* **76:** 1205–1221.

Murakami, K., Aikawa, J.I., Wada, M., Horinouchi, S., and Beppu, T. (1994) A *Mucor pusillus* mutant defective in asparagine-linked glycosylation. *J Bacteriol* **176:** 2635–2639.

Nadal, M., Garcia-Pedrajas, M.D., and Gold, S.E. (2008) Dimorphism in fungal plant pathogens. *FEMS Microbiol Lett* **284:** 127–134.

Nakatsukasa, K., Okada, S., Umebayashi, K., Fukuda, R., Nishikawa, S., and Endo, T. (2004) Roles of O-mannosylation of aberrant proteins in reduction of the load for endoplasmic reticulum chaperones in yeast. *J Biol Chem* **279:** 49762–49772.

Nemecek, J.C., Wuthrich, M., and Klein, B.S. (2006) Global control of dimorphism and virulence in fungi. *Science* **312:** 583–588.

Olson, G.M., Fox, D.S., Wang, P., Alspaugh, J.A., and Buchanan, K.L. (2007) Role of protein O-mannosyltransferase Pmt4 in the morphogenesis and virulence of *Cryptococcus neoformans*. *Eukaryot Cell* **6:** 222–234.

Prill, S.K.H., Klinkert, B., Timpel, C., Gale, C.A., Schroppel, K., and Ernst, J.F. (2005) PMT family of *Candida albicans*: five protein mannosyltransferase isoforms affect growth, morphogenesis and antifungal resistance. *Mol Microbiol* **55:** 546–560.

Rappleye, C.A., and Goldman, W.E. (2006) Defining virulence genes in the dimorphic fungi. *Annu Rev Microbiol* **60:** 281–303.

Reiss, G., Heesen, S.T., Zimmerman, J., Robbins, P.W., and Aebi, M. (1996) Isolation of the ALG6 locus of *Saccharomyces cerevisiae* required for glucosylation in the *N*-linked glycosylation pathway. *Glycobiology* **6:** 493–498.

Resheat-Eini, Z., Zelter, A., Gorovits, R., Read, N.D., and Yarden, O. (2008) The *Neurospora crassa* colonial temperature sensitive 2, 4 and 5 (*cot-2, cot-4 and cot-5*) genes encode regulatory and structural proteins required for hyphal elongation and branching. *Fungal Genet Rep* **55:** 32–36.

Richie, D.L., Hartl, L., Aimanianda, V., Winters, M.S., Fuller, K.K., Miley, M.D., *et al*. (2009) A role for the unfolded protein response (UPR) in virulence and antifungal susceptibility in *Aspergillus fumigatus*. *PloS Pathog* **5:** e1000258.

Rudd, J.J., Keon, J., and Hammond-Kosack, K.E. (2008) The wheat mitogen-activated protein kinases TaMPK3 and TaMPK6 are differentially regulated at multiple levels during compatible disease interactions with *Mycosphaerella graminicola*. *Plant Physiol* **147:** 802–815.

Rudd, J.J., Antoniw, J., Marshall, R., Motteram, J., Fraaije, B., and Hammond-Kosack, K. (2010) Identification and characterisation of *Mycosphaerella graminicola* secreted or surface-associated proteins with variable intragenic coding repeats. *Fungal Genet Biol* **47:** 19–32.

Ruddock, L.W., and Molinari, M. (2006) N-glycan processing in ER quality control. *J Cell Sci* **119:** 4373–4380.

Ruizherrera, J., Leon, C.G., Guevaraolvera, L., and Carabeztrejo, A. (1995) Yeast-mycelial dimorphism of haploid and diploid strains of *Ustilago maydis*. *Microbiology-UK* **141:** 695–703.

Sanchez-Martinez, C., and Perez-Martin, J. (2001) Dimorphism in fungal pathogens: *Candida albicans* and *Ustilago maydis* – similar inputs, different outputs. *Curr Opin Microbiol* **4:** 214–221.

Schirawski, J., Bohnert, H.U., Steinberg, G., Snetselaar, K., Adamikowa, L., and Kahmann, R. (2005) Endoplasmic reticulum glucosidase II is required for pathogenicity of *Ustilago maydis*. *Plant Cell* **17:** 3532–3543.

Schroder, M., Chang, J.S., and Kaufman, R.J. (2000) The unfolded protein response represses nitrogen-starvation induced developmental differentiation in yeast. *Genes Dev* **14:** 2962–2975.

Stolz, A., and Wolf, D.H. (2010) Endoplasmic reticulum associated protein degradation: a chaperone assisted journey to hell. *Biochim Biophys Acta-Mol Cell Res* **1803:** 694–705.

Strahl-Bolsinger, S., Gentzsch, M., and Tanner, W. (1999) Protein *O*-mannosylation. *Biochim Biophys Acta-Gen Subj* **1426:** 297–307.

Takeuchi, K., Yamazaki, H., Shiraishi, N., Ohnishi, Y., Nishikawa, Y., and Horinouchi, S. (1999) Characterization of an alg2 mutant of the zygomycete fungus *Rhizomucor pusillus*. *Glycobiology* **9:** 1287–1293.

Thiel, C., Schwarz, M., Peng, J.H., Grzmil, M., Hasilik, M., Braulke, T., *et al*. (2003) A new type of congenital disorders of glycosylation (CDG-Ii) provides new insights into the early steps of dolichol-linked oligosaccharide biosynthesis. *J Biol Chem* **278:** 22498–22505.

Timpel, C., Strahl-Bolsinger, S., Ziegelbauer, K., and Ernst, J.F. (1998) Multiple functions of Pmt1p-mediated protein *O*-mannosylation in the fungal pathogen *Candida albicans*. *J Biol Chem* **273:** 20837–20846.

Timpel, C., Zink, S., Strahl-Bolsinger, S., Schroppel, K., and Ernst, J. (2000) Morphogenesis, adhesive properties, and antifungal resistance depend on the Pmt6 protein mannosyltransferase in the fungal pathogen *Candida albicans*. *J Bacteriol* **182:** 3063–3071.

Travers, K.J., Patil, C.K., Wodicka, L., Lockhart, D.J., Weissman, J.S., and Walter, P. (2000) Functional and genomic analyses reveal an essential coordination between the unfolded protein response and ER-associated degradation. *Cell* **101:** 249–258.

Verostek, M.F., Atkinson, P.H., and Trimble, R.B. (1991) Structure of *Saccharomyces cerevisiae* Alg3, Sec18 mutant oligosaccharides. *J Biol Chem* **266:** 5547–5551.

Verostek, M.F., Atkinson, P.H., and Trimble, R.B. (1993) Glycoprotein-biosynthesis in the Alg3 *Saccharomyces cerevisiae* mutant. 1. Role of glucose in the initial glycosylation of invertase in the endoplasmic reticulum. *J Biol Chem* **268:** 12095–12103.

Whiteway, M., and Bachewich, C. (2007) Morphogenesis in *Candida albicans*. *Annu Rev Microbiol* **61:** 529–553.

Woods, J.P. (2002) *Histoplasma capsulatum* molecular genetics, pathogenesis, and responsiveness to its environment. *Fungal Genet Biol* **35:** 81–97.

Yamazaki, H., Shiraishi, N., Takeuchi, K., Ohnishi, Y., and Horinouchi, S. (1998) Characterization of alg2 encoding a mannosyltransferase in the zygomycete fungus *Rhizomucor pusillus*. *Gene* **221:** 179–184.

Zwiers, L.H., and de Waard, M.A. (2001) Efficient *Agrobacterium tumefaciens*-mediated gene disruption in the phytopathogen *Mycosphaerella graminicola*. *Curr Genet* **39:** 388–393.

Supporting information

Additional supporting information may be found in the online version of this article.

Please note: Wiley-Blackwell are not responsible for the content or functionality of any supporting materials supplied by the authors. Any queries (other than missing material) should be directed to the corresponding author for the article.